# Variational Space-time (Dis)continuous Galerkin Method for Linear Free Surface Waves

V.R. Ambati, J.J.W. van der Vegt, and O. Bokhove*

v.r.ambati@math.utwente.nl, o.bokhove@math.utwente.nl and
j.j.w.vandervegt@math.utwente.nl

Numerical Analysis and Computational Mechanics Group
Department of Applied Mathematics, University of Twente
P.O. Box 217, Enschede, The Netherlands.

March 5, 2008

### Abstract

A new variational (dis)continuous Galerkin finite element method is presented for linear free surface gravity water wave equations. In this method, the space-time finite element discretization is based on a discrete variational formulation analogous to a version of Luke's variational principle. The finite element discretization results into a linear algebraic system of equations with a symmetric and compact stencil. These equations have been solved using the PETSc package, in which a block sparse matrix storage routine is used to build the matrix and an efficient conjugate gradient solver to solve the equations. The finite element scheme is verified against exact solutions: linear free surface waves in a periodic domain and ones generated by a harmonic wave maker in a rectangular wave basin. We found that the variational scheme has no dissipation and minimal dispersion errors in the wave propagation, and that the numerical results obtained are $(p+1)$-order accurate for a $p^{\text{th}}$-order polynomial approximation of the wave field.

*Keywords:* Finite element methods, Discontinuous Galerkin methods, Free Surface Waves, Variational Principle.
*Mathematics Subject Classification:* 65M60, 65N30, 76B07, 76B15.

## 1 Introduction

A large class of water wave problems is captured by a model that consists of a potential flow equation coupled with nonlinear free surface boundary conditions. These equations are obtained from the Euler equations of fluid motion with the assumptions that the fluid is inviscid and incompressible, and the velocity field irrotational (see Johnson [8]). This model proves useful in studying many marine and offshore engineering problems such as the wave induced motion of ships and the control of wave generation by wave makers in laboratory basins.

The free surface gravity water wave equations are obtained in a succinct way via Luke's variational principle [13] or from its dynamical equivalent presented by Miles [18]. The essence of the variational principle is that the complete problem can be expressed in a single functional. In addition, the variational formulation is associated with the conservation of energy and phase space, under suitable boundary conditions. Variational formulations also provide a basis for the construction of approximate finite element solutions. Such variational finite element methods for free surface waves

---

*Corresponding Authors: Vijaya Ambati and Onno Bokhove; o.bokhove@math.utwente.nl

can be found in Bai and Kim [3], Kim and Bai [9] and Kim et al. [10]. Klopman et al. [11] derive a variational Boussinesq model from Luke's variational principle; in essence their Boussinesq model is a vertical discretization thereof. It motivated us to investigate a (dis)continuous Galerkin finite element method based on a discretization of Luke's variational principle. Such a discretization aims to preserve the variational structure and the associated energy and phase-space conservation.

Standard finite element element methods for free surface gravity water waves are relatively new and can be found in [7, 14, 15, 16, 28, 30, 31]. Another widely used numerical method for free surface waves is the boundary integral method which started with the work of Longuet-Higgins and Cokelet [12], and Vinje and Brevig [27]. This method has been applied extensively to two dimensional free surface waves, see the surveys of Romate [19] and Tsai and Yue [23]. Applications in three dimensions (3D) using boundary integral methods include [6, 19, 4]. The discontinuous Galerkin (DG) methods for elliptic problems proposed by Arnold et al. [2] and Brezzi [5] have enabled researchers to model free surface water waves using a space discontinuous Galerkin method. A space(-time) DG finite element method for free surface wave problems has been developed in Van der Vegt and Tomar [24]. and Van der Vegt and Xu [26]. However, a conservative DG method for free surface waves based on its variational formulation appears to be non-existent.

Nonlinear free surface gravity water wave equations are difficult to solve because the solution to the governing equations depends on the position of the free surface which is not known apriori. To deal with such difficulties, we choose a space-time approach which is particularly well-suited for problems with time dependent boundaries (see Van der Vegt and Van der Ven [25], Ambati and Bokhove [1], Van der Vegt and Xu [26]).

General reasons to employ DG methods are as follows:

**(i)** the scheme is local in the sense that the solution in each element only depends on its neighboring elements via the flux through element boundaries and is thus suitable for parallelization; and,

**(ii)** the scheme is extendable to have hp–adaptivity in which the fluid flow field approximation can arbitrarily vary per element, known as "p–adaptivity", and the mesh can be locally refined, called "h–adaptivity".

An accurate space-time DG finite element scheme for water waves has potential and is challenging because

**(i)** it is less trivial to develop an efficient solution technique for the nonlinear algebraic equations resulting from the discretization, and

**(ii)** it is a natural, yet more involved approach to handle the grid deformation due to the nonlinear free surface evolution.

We therefore first consider the development of a variational space-time (dis)continuous Galerkin finite element method (DGFEM) for linear free surface gravity water waves based on Luke's variational principle.

The linear free surface gravity water wave problem, in essence, consists of two second-order differential equations for the velocity potential, in which one equation has a second-order spatial derivative and the other one a second-order time derivative. The discontinuous Galerkin formulation for an elliptic problem proposed by Brezzi et al. [5] is symmetric and, hence, a discrete variational formulation could be deduced from it. However, a discontinuous Galerkin variational formulation for the second-order time derivative is less trivial. We therefore first present a discrete variational formulation for a harmonic oscillator as a building block. Subsequently, we combine these two discrete variational formulations to obtain a variational space-time DG method for linear free surface water waves.

In a variational space-time (dis)continuous Galerkin method, the domain is split into space-time slabs which are tessellated with space-time finite elements. On these elements, we define local basis functions to approximate the wave field and also the test functions and variations. The local basis functions are defined such that the approximation of the wave field is discontinuous in space, but

continuous in time. This kind of approximation is mainly chosen to satisfy the requirement of zero variation of the velocity potential at the end points in time.

The space-time variational formulation for our problem is obtained in two steps. In the first step, we establish a relation between the velocity field and velocity potential through the primal formulation given in Arnold et al. [2] and Brezzi et al. [5]. In the second step, we introduce a discrete version variational principle, analogous to the continuum functional for linear free surface waves. Subsequently, we take variations to obtain the discretization for the linear free surface wave problem.

The space-time discretization of the discrete variational formulation for linear free surface waves results into a linear algebraic system of equations. The global matrix of this linear system has a very compact stencil, *i.e.,* the number of non-zero entries in each row of the matrix only depends on the number of neighbors of an element. Further, the linear system is symmetric and we can therefore use an efficient sparse matrix storage routine and an (iterative) sparse linear solver. The need to use efficient solvers led us to the PETSc package (see [20, 21, 22]) for assembling and solving our linear system of algebraic equations. The software library of PETSc has a large suite of well-tested sparse matrix storage routines and (iterative) sparse linear solvers with the extra advantage of parallelization options. Hence, we have incorporated the PETSc package in our numerical implementation. Within PETSc, we have used an efficient block sparse matrix storage routine for assembling the global matrix and a conjugate-gradient solver with ILU preconditioner for solving the linear system.

We have compared the variational space-time (dis)continuous Galerkin method with the "standard" space-time discontinuous Galerkin method developed by van der Vegt and Xu [26]. Hence, we also discuss the space-time discontinuous Galerkin method, which numerical implementation we extended to three space dimensions. The numerical results from both the variational and standard space-time (dis)continuous Galerkin methods are compared with two exact solutions: linear harmonic waves in a periodic domain and linear waves generated in a wave basin. We found for these three dimensional test cases that both the numerical schemes are second- and third-order accurate for a linear and quadratic polynomial approximations of the wave field.

The paper unfolds as follows. To start, a time discrete variational formulation is investigated first for a harmonic oscillator in §4.2. We present a variational formulation for the linear free surface wave problem and subsequently derive the governing equations in §4.3. Technicalities, the tessellation of the space-time domain and the required function spaces and trace operators for the space-time finite element formulations, are defined in §4.4. Next, we present the standard and variational space-time (dis)continuous Galerkin finite element formulations of the linear free surface wave problem next in §4.5 and §4.6, respectively. Numerical results of both schemes are compared with exact solutions in §4.7. Conclusions are drawn in §4.8.

## 2    Variational discretization for a harmonic oscillator

The dynamics of a harmonic oscillator is contained in the following functional in time:

$$L(\phi, \eta) := \int_0^T \phi \partial_t \eta \mathrm{d}t - \int_0^T \frac{1}{2}(\omega^2 |\phi|^2 + \eta^2) \mathrm{d}t \tag{1}$$

with $\phi(t)$ the position, $\eta(t)$ the velocity and $\omega$ the constant frequency of the oscillator in the time interval $[0, T]$. Applying the variational principle $\delta L = 0$, we obtain:

$$\int_0^T \left( \delta\phi \, \partial_t \eta + \phi \, \partial_t(\delta\eta) \right) \mathrm{d}t - \int_0^T (\omega^2 \phi \, \delta\phi + \eta \, \delta\eta) \mathrm{d}t = 0. \tag{2}$$

Integrating (2) by parts, while using the end-point conditions $\delta\eta(0) = \delta\eta(T) = 0$, for the variation $\delta\eta$, and the arbitrariness of the variations; the dynamics of a harmonic oscillator emerge as

$$\partial_t \eta - \omega^2 \phi = 0 \quad \text{and} \quad \partial_t \phi + \eta = 0; \tag{3}$$

initial conditions are $\phi(t = 0) = \phi_0$ and $\eta(t = 0) = \eta_0$.

Combining the governing equations of a harmonic oscillator in (3), we obtain a second-order equation for $\phi$. The discontinuous Galerkin formulation for such a second-order time derivative may be different to that of a symmetric second-order spatial derivative following the approach of Brezzi et al. [5]. The difference mainly arises due to the definition of numerical flux, often a kind of upwind flux for time derivatives and central flux for spatial derivatives. As a consequence, the DG formulation for harmonic oscillator is not automatic in symmetric form, and does not stem from a discrete variational formulation. A discrete variational formulation for the harmonic oscillator is therefore obtained by choosing a continuous approximation of functions $\phi$ and $\eta$ in time.

To formulate a discrete variational formulation for the harmonic oscillator, we first divide the time domain into finite time intervals $I_n = [t_{n-1}, t_n]$. Each time interval $I_n$ is then related to a fixed interval $\hat{I} = \zeta \in [-1, 1]$ through the mapping $F_n$ defined as

$$F_n : \hat{I} \to I_n : \zeta \mapsto t = \frac{1}{2}\big(t_{n-1}(1 - \zeta) + t_n(1 + \zeta)\big). \tag{4}$$

Next, the functions $\phi$ and $\eta$ are approximated as

$$\phi_{\mathsf{h}} = \phi_n \psi_n + \phi_{n-1}\psi_{n-1} \quad \text{and} \quad \eta_{\mathsf{h}} = \eta_n \psi_n + \eta_{n-1}\psi_{n-1}, \tag{5}$$

where $\psi_n \circ F_n = (1 + \zeta)/2$ and $\psi_{n-1} \circ F_n = (1 - \zeta)/2$ are the tent functions; and, $(\phi_n, \eta_n)$ and $(\phi_{n-1}, \eta_{n-1})$ are the nodal values of $(\phi_{\mathsf{h}}, \eta_{\mathsf{h}})$ at times $t_n$ and $t_{n-1}$, respectively.

The discrete functional for the harmonic oscillator, analogous to (1), is taken as

$$L_{\mathsf{h}}(\phi_{\mathsf{h}}, \eta_{\mathsf{h}}) := \int_{t_{n-1}}^{t_n} \phi_{\mathsf{h}} \partial_t \eta_{\mathsf{h}} \mathrm{d}t - \int_{t_{n-1}}^{t_n} \frac{1}{2}(\omega^2 |\phi_{\mathsf{h}}|^2 + \eta_{\mathsf{h}}^2)\mathrm{d}t \tag{6}$$

for each time interval $I_n$. Applying the variational principle $\delta L_{\mathsf{h}} = 0$ and using the arbitrariness of variations, the discrete variational formulation for the harmonical oscillator is obtained as follows: Find a $\phi_n$ and $\eta_n$ for given $\phi_{n-1}$ and $\eta_{n-1}$ such that for all $\delta\phi$ and $\delta\eta$ equations

$$\int_{t_{n-1}}^{t_n} \Big((\partial_t \eta_{\mathsf{h}})\delta\phi_{\mathsf{h}} - \omega^2 \phi_{\mathsf{h}}\delta\phi_{\mathsf{h}}\Big)\mathrm{d}t = 0 \quad \text{and} \quad \int_{t_{n-1}}^{t_n} \Big(\phi_{\mathsf{h}}\partial_t(\delta\eta_{\mathsf{h}}) - \eta_{\mathsf{h}}\delta\eta_{\mathsf{h}}\Big)\mathrm{d}t = 0 \tag{7}$$

are satisfied with the end point conditions $\delta\phi(t_n) = \delta\phi(t_{n-1}) = \delta\eta(t_n) = \delta\eta(t_{n-1}) = 0$.

The variational time finite element discretization is obtained by substituting the approximations (5) into (7) and by choosing the rather special variations $\delta\phi_{\mathsf{h}} = \delta\eta_h = \psi_n\psi_{n-1}$ such that they vanish at the end points. The result is

$$\frac{\eta_n - \eta_{n-1}}{\Delta t} = \omega^2 \Big(\frac{\phi_n + \phi_{n-1}}{2}\Big) \quad \text{and} \quad \frac{\phi_n - \phi_{n-1}}{\Delta t} = -\Big(\frac{\eta_n + \eta_{n-1}}{2}\Big) \tag{8}$$

with $\Delta t = t_n - t_{n-1}$. The discretization in (8) corresponds to a mid point scheme which is known to be energy conserving. Consequently, in Fig. 1, we see that there is no decay in the amplitude of the numerical solution when compared with the exact solution. However, we observe a dispersion error which decreases for smaller time steps. Later in this paper, we also use the present time discretization technique in the variational space-time discontinuous Galerkin finite element method for linear free surface waves.

## 3  Linear free surface gravity water waves

In fluid dynamics, the governing equations for free surface gravity water waves are derived from the incompressible Euler equations of fluid motion (see Johnson [8] or Whitham [29]). These governing equations can, however, also be derived from Luke's or Miles' variational principle [13, 18]. The advantage of using this principle is that the governing equations are obtained from a single energy functional. Conservation laws are thus directly associated with this variational principle via Noether's theorem. A direct discretization of the variational principle is then also advantageous. We therefore derive the linear free surface gravity water wave equations from a variational principle.
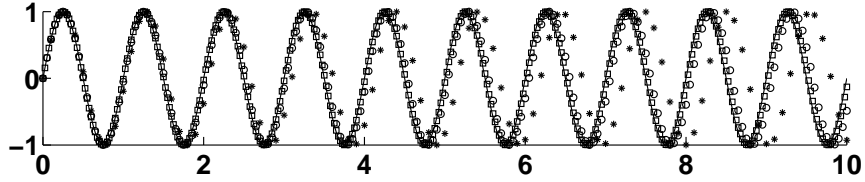
Figure 1: Comparsion of exact (solid line) and numerical (stars, circles and squares) solutions with initial conditions $\phi_0 = 0$ and $\eta_0 = -\omega = -2\pi$. The exact solution is $\phi = \sin(\omega t)$ and the numerical solutions are computed with time steps $\Delta t = 0.1$ (stars), 0.05 (circles) and 0.025 (squares).

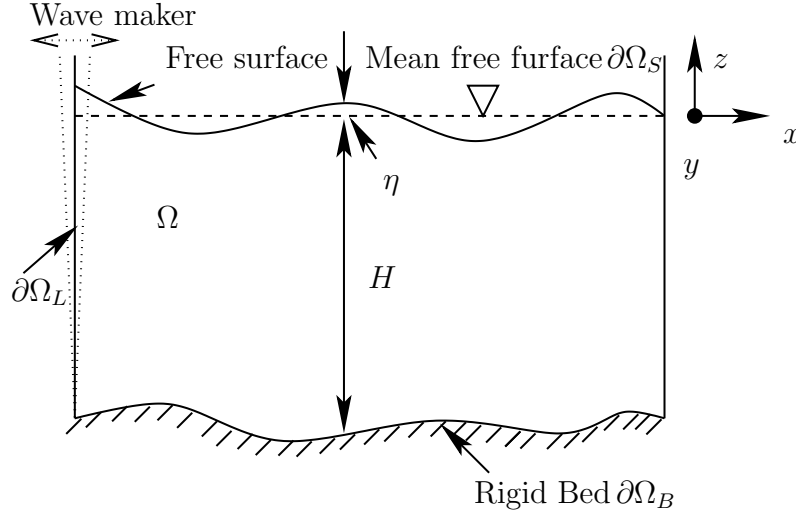## 3.1 Variational principle for linear water waves



Figure 2: A sketch of the domain and its boundaries for the linear water wave problem including the waves generated by a wave maker. The flat mean free surface (top) and the mean wall position (left) of the wave maker arise as the fixed, reference boundaries after linearization of the nonlinear free surface and wave maker motions.

Consider an incompressible and inviscid fluid in a domain $\Omega \subset \mathbf{R}^3$ with boundaries $\partial\tilde{\Omega} = \partial\tilde{\Omega}_S \cup \partial\Omega_B \cup \partial\tilde{\Omega}_L$ as shown in Fig. 2, where $\partial\tilde{\Omega}_S$ is the free surface, $\partial\Omega_B$ the rigid bed, and $\partial\tilde{\Omega}_L$ denotes lateral boundaries. Assuming a non-overturning free surface, we parameterize the free surface as $z = \eta(t, x, y)$, where $\eta(t, x, y)$ is a perturbation of the free surface around a mean free surface located at $z = 0$ and measured at a height $H(x, y)$ from the rigid bottom surface $\partial\Omega_B$.

For free surface gravity water waves, it is justified to assume the flow field to be irrotational. Hence, $\mathbf{u} = \bar{\nabla}\phi$ such that $\bar{\nabla} \times \mathbf{u} = 0$ with $\bar{\nabla} = (\partial_x, \partial_y, \partial_z)^T$, $\mathbf{u} = (u, v, w)$ the velocity field, and $u$, $v$ and $w$ the components of the velocity in the $x$, $y$ and $z$ direction, respectively. We assume the perturbations of the free surface wave height $\eta$ and the velocity potential $\phi$ to be of small amplitude. After linearization, the mean free surface $\partial\Omega_S$ instead of actual free surface and solid (vertical) walls $\partial\Omega_L$ instead of the wave makers emerge as the boundary $\partial\Omega$ of the flow domain (see Fig. 2) for the linearized equations of motion.

To facilitate the variational calculus, we first introduce a horizontal cross section of the flow domain $\Omega$ as $\bar{\Omega}(z)$ such that the flow domain $\Omega$ is defined by

$$\Omega := \{(x, y, z) | \ 0 < z < -H \text{ and } (x, y) \in \bar{\Omega}(z)\}. \tag{9}$$

Next, we define the kinetic energy $E_K$ and potential energy $E_P$ of the waves in $\Omega$ as

$$E_K := \int_\Omega \frac{1}{2}|\bar{\nabla}\phi|^2 \, \mathrm{d}\Omega - \int_{\partial\Omega_L} g_N\phi \, \mathrm{d}(\partial\Omega) \quad \text{and} \quad E_P := \int_{\partial\Omega_S} \frac{1}{2}g\eta^2 \, \mathrm{d}x \, \mathrm{d}y \tag{10}$$

with $g$ the gravitational acceleration in the vertical and $g_N$ a prescribed normal velocity at the lateral boundaries. The functional for linear free surface waves then reads

$$\mathcal{L}_f(\phi, \phi_s, \eta) = \int_0^T \int_{\partial\Omega_S} \phi_s \partial_t \eta \, \mathrm{d}x \, \mathrm{d}y \, \mathrm{d}t - \int_0^T (E_K + E_P) \, \mathrm{d}t \tag{11}$$

with $T$ the final time, and $\phi_s(x, y, t) = \phi(x, y, z = 0, t)$ the velocity potential evaluated at the mean free surface. The functional $\mathcal{L}_f(\phi, \phi_s, \eta)$ for the nonlinear case was originally defined by Luke [13] and Miles [18].

Finally, the variational formulation for linear free surface waves becomes:

$$\delta\mathcal{L}_f(\phi, \phi_s, \eta) = 0, \tag{12}$$

where $\delta\mathcal{L}_f(\phi, \phi_s, \eta)$ is the variational derivative defined as

$$\delta\mathcal{L}_f(\phi, \phi_s, \eta) := \lim_{\epsilon \to 0} \frac{1}{\epsilon}\big(\mathcal{L}_f(\phi + \epsilon\delta\phi, \phi_s + \epsilon\delta\phi_s, \eta + \epsilon\delta\eta) - \mathcal{L}_f(\phi, \phi_s, \eta)\big) \tag{13}$$

with $\delta\phi, \delta\phi_s$ and $\delta\eta$ arbitrary variations of $\phi, \phi_s$ and $\eta$, respectively. The variational formulation (10)–(12) will form the basis to obtain a variational (dis)continuous Galerkin finite element discretization.

Applying the variational principle (10)–(12) and using the definition of the variational derivative (13), we obtain

$$\int_0^T \Big( \int_{\partial\Omega_S} \big(\delta\phi_s \partial_t \eta + \phi_s \partial_t \delta\eta - g\eta\delta\eta\big) \, \mathrm{d}x \, \mathrm{d}y - \int_\Omega \bar{\nabla}\phi \cdot \bar{\nabla}\delta\phi \, \mathrm{d}\Omega + \int_{\partial\Omega_L} g_N\delta\phi \, \mathrm{d}(\partial\Omega)\Big) \, \mathrm{d}t = 0. \tag{14}$$

To obtain the governing equations for linear free surface waves from (14), we integrate the second term by parts in time, use Gauss' divergence theorem for the third term, and rearrange the emerging boundary integrals in time using the following end-point conditions on the variation: $\delta\eta(x, y, 0) = \delta\eta(x, y, T) = 0$. Hence, from (14) we derive

$$\int_0^T \Big( \int_{\partial\Omega_S} \big( -(\partial_t\phi_s + g\eta)\delta\eta + (\partial_t\eta - \partial_z\phi)\delta\phi_s \big) \, \mathrm{d}x \, \mathrm{d}y + \int_\Omega \bar{\nabla}^2\phi \, \delta\phi \, \mathrm{d}\Omega$$

$$- \int_{\partial\Omega_L} (\tilde{n}_L \cdot \bar{\nabla}\phi - g_N)\delta\phi \, \mathrm{d}(\partial\Omega) - \int_{\partial\Omega_B} (\tilde{\mathbf{n}}_B \cdot \bar{\nabla}\phi)\delta\phi \, \mathrm{d}(\partial\Omega) \Big) \mathrm{d}t = 0, \tag{15}$$

where $\tilde{\mathbf{n}}_L = (\pm 1, 0, 0)^T$ and $\tilde{\mathbf{n}}_B$ are the outward unit normal vectors at the boundaries $\partial\Omega_L$ and $\partial\Omega_B$, respectively. Using the arbitrariness of the variations $\delta\phi$, $\delta\phi_s$ and $\delta\eta$ in (15), the governing equations for linear free surface gravity water waves emerge as

$$\bar{\nabla}^2\phi = 0 \quad \text{on} \quad \Omega(t),$$
$$\partial_t\eta - \partial_z\phi = 0 \quad \text{and} \quad \partial_t\phi_s + g\eta = 0 \text{ on } \partial\Omega_S,$$
$$\tilde{\mathbf{n}}_L \cdot \bar{\nabla}\phi = g_N \text{ on } \partial\Omega_L, \quad \text{and} \quad \tilde{\mathbf{n}}_B \cdot \bar{\nabla}\phi = 0 \text{ on } \partial\Omega_B. \tag{16}$$

# 4 Basis for space-time formulation

## 4.1 Space-time domain and tessellation

In space-time discontinuous Galerkin methods, we do not distinguish between space and time, and directly define the space-time flow domain $\mathcal{E} \in \mathbb{R}^4$ as

$$\mathcal{E} := \{\mathbf{x} \in \mathbb{R}^4 : \bar{\mathbf{x}} \in \Omega, t_0 < t < T)\} \subseteq \mathbb{R}^4 \tag{17}$$

6

with $\mathbf{x} = (t, \mathbf{x})$ the space-time coordinates, $\bar{\mathbf{x}} = (x, y, z)$ the spatial coordinates, $t_0$ the initial time, $T$ the final time and $\Omega \in \mathbb{R}^3$ the flow domain. The space-time boundary $\partial \mathcal{E}$ consists of the hypersurfaces $\Omega_0 := \{\mathbf{x} \in \partial \mathcal{E} : t = t_0\}$, $\Omega_T := \{\mathbf{x} \in \partial \mathcal{E} : t = T\}$ and $\mathcal{Q} := \{\mathbf{x} \in \partial \mathcal{E} : t_0 < t < T\}$. The unit outward space-time normal vector of the space-time domain boundary is defined as $\mathbf{n} := (n_t, \bar{\mathbf{n}})$ with $n_t$ the temporal component and $\bar{\mathbf{n}}$ the spatial component.

To tessellate the space-time domain $\mathcal{E}$, we first divide the time interval $I = [t_0, T]$ into $N_T$ time intervals with each time interval denoted as $I_n = [t_{n-1}, t_n]$. Second, at each time level $t_n$, we tessellate the flow domain $\Omega$ with $N_e$ shape regular spatial elements $K_k^n$ to form a computational flow domain $\Omega_h$ such that $\Omega_h \to \Omega$ as $h \to 0$, where $h$ is the radius of the smallest sphere containing all elements $K_k^n$ with $k = 1, \ldots, N_e$. Finally, in each time interval $I_n$, we obtain the space-time tessellation $\mathcal{T}_h^n$ for the computational space-time domain $\mathcal{E}_h^n$ which consists of the space-time elements $\mathcal{K}_k^n$ obtained by joining the spatial elements $K_k^{n-1}$ and $K_k^n$ at the successive time intervals $t_{n-1}$ and $t_n$. For linear free surface waves, the computational flow domain $\Omega_h$ is fixed in time and hence the corresponding spatial elements $K_k^{n-1}$ and $K_k^n$ of the space-time element $\mathcal{K}_k^n$ are identical. Hereafter, we thus drop the superscript $n$ of the spatial element.

To define function spaces and apply quadrature rules, each spatial element $K_k$ is mapped onto a reference element $\hat{K}$ and its mapping $F_K : \hat{K} \to K_k$ is defined as

$$F_K : \hat{K} \to K_k : \bar{\zeta} \mapsto \bar{\mathbf{x}} := \sum_j \bar{\mathbf{x}}_j \, \chi_j(\bar{\zeta}) \tag{18}$$

with $\bar{\zeta} = (\zeta_1, \zeta_2, \zeta_2)$ the spatial reference coordinates, $\bar{\mathbf{x}} = (x, y, z)$ the spatial coordinates, $\bar{\mathbf{x}}_j$ the nodal coordinates of the spatial element and $\chi_j(\bar{\zeta})$ the standard shape functions of element $K_k$. Subsequently, the space-time element $\mathcal{K}_k^n$ is mapped to a reference element $\hat{\mathcal{K}}$ and its mapping is defined as

$$G_\mathcal{K}^n : \hat{\mathcal{K}} \to \mathcal{K}_k^n : \zeta \mapsto \mathbf{x} := \left( \frac{1}{2}\big((1 + \zeta_0)t_n + (1 - \zeta_0)t_{n-1}\big), F_K(\bar{\zeta}) \right) \tag{19}$$

with $\zeta = (\zeta_0, \bar{\zeta})$ the space-time reference coordinates.

In the space-time tessellation $\mathcal{T}_h^n$, we further define interior faces $\mathcal{S}_{int}$, which connect two space-time elements $\mathcal{K}_l^n$ and $\mathcal{K}_r^n$, and boundary faces $\mathcal{S}_{bou}$ which connect space-time elements $\mathcal{K}_l^n$ to the boundary $\partial \mathcal{E}$. The union of all faces in the space-time domain $\mathcal{E}_h^n$ is represented as $\Gamma = \Gamma_{int} \cup \Gamma_{bou}$, with $\Gamma_{int}$ the union of interior faces and $\Gamma_{bou}$ the union of boundary faces. The union of boundary faces $\Gamma_{bou} := \Gamma_S \cup \Gamma_B \cup \Gamma_L$ further consists of $\Gamma_S$ the union of free surface faces, $\Gamma_B$ the union of rigid boundary faces, and $\Gamma_L$ the union of lateral boundary faces of the computational space-time domain $\mathcal{E}_h^n$ which may include the linearized wave maker.

## 4.2 Function spaces

To define the space-time discontinuous Galerkin formulation, we introduce the finite element function spaces $V_h$ and $\Sigma_h$, associated with the space-time tessellation $\mathcal{T}_h^n$, which are defined as

$$V_h := \{v_h \in L^2(\mathcal{E}_h^n) : \ v_h \circ G_\mathcal{K}^n \in \mathcal{P}_p(\hat{\mathcal{K}}), \ \forall \mathcal{K}_k^n \in \mathcal{T}_h^n\},$$
$$\Sigma_h := \{\tau_h \in L^2(\mathcal{E}_h^n) : \ \tau_h \circ G_\mathcal{K}^n \in [\mathcal{P}_p(\hat{\mathcal{K}})]^3, \ \forall \mathcal{K}_k^n \in \mathcal{T}_h^n\} \tag{20}$$

with $L^2(\mathcal{E}_h^n)$ the space of Lebesgue square integrable functions on $\mathcal{E}_h^n$ and $\mathcal{P}_p$ (space-time) polynomials of order $p$. We also introduce the function space $W_h$ associated with the space-time free surface $\Gamma_S$ which is defined as

$$W_h := \{v_h \in L^2(\Gamma_S) : \ v_h \circ G_\mathcal{K} \in \mathcal{P}_p(\hat{\mathcal{S}}), \ \forall \mathcal{S} \subset \Gamma_S\}, \tag{21}$$

with $\hat{\mathcal{S}}$ a face of $\hat{\mathcal{K}}$ and $L^2(\Gamma_S)$ the space of Lebesgue square integrable functions on the space-time free surface boundary $\Gamma_S$.

For the space-time discontinuous Galerkin formulation, we approximate flow fields $(\mathbf{u}, \phi, \eta)$ as

$$\phi_{\mathsf{h}} = \sum_{j=1}^{n_p} \hat{\phi}_{\mathsf{k},j} \psi_{\mathsf{k},j}, \quad \mathbf{u}_{\mathsf{h}} = \sum_{j=1}^{n_p} \hat{\mathbf{u}}_{\mathsf{k},j} \psi_{\mathsf{k},j} \quad \text{and} \quad \eta_{\mathsf{h}} = \sum_{j=1}^{n_q} \hat{\eta}_{\mathsf{k},j} \varphi_{\mathsf{k},j}, \tag{22}$$

with $\phi_{\mathsf{h}} \in V_{\mathsf{h}}$, $\mathbf{u}_{\mathsf{h}} \in \Sigma_{\mathsf{h}}$ and $\eta_{\mathsf{h}} \in W_{\mathsf{h}}$ the approximated wave fields; $(\hat{\phi}_{\mathsf{k},j}, \hat{\mathbf{u}}_{\mathsf{k},j}, \hat{\eta}_{\mathsf{k},j})$ the expansion coefficients; $\psi_{\mathsf{k},j} \circ G_{\mathcal{K}}^n \in \mathcal{P}_p(\hat{\mathcal{K}})$ and $\varphi_{\mathsf{k},j} \circ G_{\mathcal{K}}^n \in \mathcal{P}_p(\hat{\mathcal{S}})$ the polynomial basis functions; and, $n_p$ and $n_q$ the number of basis functions in the space-time elements and at the space-time free surface, respectively.

To define the space-time variational formulation, we introduce the finite element function spaces $\bar{V}_{\mathsf{h}}$ and $\bar{\Sigma}_{\mathsf{h}}$ associated with the computational space domain $\Omega_{\mathsf{h}}$ which are defined as

$$\bar{V}_{\mathsf{h}} := \{\bar{v}_{\mathsf{h}} \in L^2(\Omega_{\mathsf{h}}) : \ \bar{v}_{\mathsf{h}} \circ F_K \in \mathcal{P}_p(\hat{K})\},$$
$$\bar{\Sigma}_{\mathsf{h}} := \{\bar{\tau}_{\mathsf{h}} \in L^2(\Omega_{\mathsf{h}}) : \ \bar{\tau}_{\mathsf{h}} \circ F_K \in [\mathcal{P}_p(\hat{K})]^3\}, \tag{23}$$

where $L^2(\Omega_{\mathsf{h}})$ is the space of Lebesgue square integrable functions on $\Omega_{\mathsf{h}}$ and $\mathcal{P}_p$ the (space) polynomials of order $p$. We also introduce the function space $\bar{W}_{\mathsf{h}}$ associated with the free surface $\partial\Omega_S$ which is defined as

$$\bar{W}_{\mathsf{h}} := \{\bar{v}_{\mathsf{h}} \in L^2(\partial\Omega_S) : \ \bar{v}_{\mathsf{h}} \circ F_K \in \mathcal{P}_p(\hat{S})\} \tag{24}$$

with $\hat{S}$ a face of $\hat{K}$ and $L^2(\partial\Omega_S)$ the space of Lebesgue square integrable functions on the free surface $\partial\Omega_S$.

For the space-time variational formulation, we first approximate the flow field $(\mathbf{u}, \phi, \eta)$ on the computational space domain $\Omega_{\mathsf{h}}$ at time level $t_n$ as

$$\bar{\phi}_{\mathsf{h}}^n = \sum_{j=1}^{n_p} \hat{\phi}_{\mathsf{k},j}^n \bar{\psi}_{\mathsf{k},j}, \quad \bar{\mathbf{u}}_{\mathsf{h}}^n = \sum_{j=1}^{n_p} \hat{\mathbf{u}}_{\mathsf{k},j}^n \bar{\psi}_{\mathsf{k},j} \quad \text{and} \quad \bar{\eta}_{\mathsf{h}}^n = \sum_{j=1}^{n_q} \hat{\eta}_{\mathsf{k},j}^n \bar{\varphi}_{\mathsf{k},j} \tag{25}$$

with $\bar{\phi}_{\mathsf{h}}^n, \bar{\mathbf{u}}_{\mathsf{h}}^n, \bar{\eta}_{\mathsf{h}}^n$ the approximated flow fields; $(\hat{\phi}_{\mathsf{k},i}^n, \hat{\mathbf{u}}_{\mathsf{k},i}^n, \hat{\eta}_{\mathsf{k},j}^n)$ the expansion coefficients; $\bar{\psi}_{\mathsf{k},j} \circ F_K \in \mathcal{P}_p(\hat{K})$ and $\bar{\varphi}_{\mathsf{k},j} \circ F_K^n \in \mathcal{P}_p(\hat{S})$ the polynomial basis functions; and, $n_p$ and $n_q$ the number of basis functions in the spatial element and at the free surface, respectively.

Second, we define the polynomial basis functions in time $\psi^{n-1}$ and $\psi^n$ as follows

$$\psi^{n-1} := \frac{1}{2}(1 - \zeta_0)t_{n-1} \quad \text{and} \quad \psi^n := \frac{1}{2}(1 + \zeta_0)t_n. \tag{26}$$

Finally, we obtain the approximation of the wave field on each space-time element $\mathcal{K}_{\mathsf{k}}^n$ as

$$(\phi_{\mathsf{h}}, \mathbf{u}_{\mathsf{h}}, \eta_{\mathsf{h}}) = (\bar{\phi}_{\mathsf{h}}^n, \bar{\mathbf{u}}_{\mathsf{h}}^n, \bar{\eta}_{\mathsf{h}}^n)\psi^n + (\bar{\phi}_{\mathsf{h}}^{n-1}, \bar{\mathbf{u}}_{\mathsf{h}}^{n-1}, \bar{\eta}_{\mathsf{h}}^{n-1})\psi^{n-1} \tag{27}$$

with $\bar{\phi}_{\mathsf{h}} \in \bar{V}_{\mathsf{h}}$, $\bar{\mathbf{u}}_{\mathsf{h}} \in \bar{\Sigma}_{\mathsf{h}}$ and $\bar{\eta}_{\mathsf{h}} \in \bar{W}_{\mathsf{h}}$ and the restriction that the approximation is continuous in time but discontinuous in space.

## 4.3 Traces

To define and manipulate the numerical fluxes in the discontinuous Galerkin formulation, we define the traces of functions $v \in V_{\mathsf{h}}$ and vector functions $\mathbf{q} \in \Sigma_{\mathsf{h}}$ on the element boundary $\partial\mathcal{K}_{\mathsf{k}}^n$ taken from inside of the element $\mathcal{K}_{\mathsf{k}}^n$ as

$$v_{\mathsf{h}}|_{\partial\mathcal{K}_{\mathsf{k}}^n} := v^- = \lim_{\epsilon\downarrow 0} v(\mathbf{x} - \epsilon\mathbf{n}_{\mathcal{K}}) \ \text{and} \ \mathbf{q}_{\mathsf{h}}|_{\partial\mathcal{K}_{\mathsf{k}}^n} := \mathbf{q}^- := \lim_{\epsilon\downarrow 0} \mathbf{q}(\mathbf{x} - \epsilon\mathbf{n}_{\mathcal{K}}) \tag{28}$$

with $n_{\mathcal{K}}$ the unit outward normal vector of the element boundary $\partial\mathcal{K}_{\mathsf{k}}^n$. For convenience, we also denote the traces $v^-$ and $\mathbf{q}^-$ on $\partial\mathcal{K}_{\mathsf{k}}^n$ as $v_{\mathsf{k}}$ and $\mathbf{q}_{\mathsf{k}}$, respectively. Now, we define the following trace operators:

**Average** The averages $\{\!\{v\}\!\}$ of a scalar function $v \in V_\mathsf{h}$ and $\{\!\{\mathbf{q}\}\!\}$ of a vector function $\mathbf{q} \in \Sigma_\mathsf{h}$ on a face $\mathcal{S} \in \Gamma$ are defined as

$$
\begin{aligned}
\{\!\{v\}\!\} &:= \frac{1}{2}(v_\mathsf{l} + v_\mathsf{r}), & \{\!\{\mathbf{q}\}\!\} &:= \frac{1}{2}(\mathbf{q}_\mathsf{l} + \mathbf{q}_\mathsf{r}) & \forall \mathcal{S} \in \Gamma_{int}; \text{ and} \\
\{\!\{v\}\!\} &:= v_\mathsf{l}, & \{\!\{\mathbf{q}\}\!\} &:= \mathbf{q}_\mathsf{l} & \forall \mathcal{S} \in \Gamma_{bou}
\end{aligned}
\tag{29}
$$

with $v_\mathsf{l}$ and $v_\mathsf{r}$ the traces of the scalar function $v_\mathsf{h}$, and $\mathbf{q}_\mathsf{l}$ and $\mathbf{q}_\mathsf{r}$ the traces of the vector function $\mathbf{q}_\mathsf{h}$ taken from the inside of the elements $\mathcal{K}_\mathsf{l}^n$ and $\mathcal{K}_\mathsf{r}^n$ connected at the face $\mathcal{S}$.

**Jump** The jumps $[\![v]\!]$ of a scalar function $v \in V_\mathsf{h}$ and $[\![\mathbf{q}]\!]$ of a vector function $\mathbf{q} \in \Sigma_\mathsf{h}$ on a face $\mathcal{S} \in \Gamma$ are defined as

$$
\begin{aligned}
[\![v]\!] &:= v_\mathsf{l}\bar{\mathbf{n}}_\mathcal{K}^\mathsf{l} + v_r\bar{\mathbf{n}}_\mathcal{K}^r, & [\![\mathbf{q}]\!] &:= \mathbf{q}_\mathsf{l} \cdot \bar{\mathbf{n}}_\mathcal{K}^\mathsf{l} + \mathbf{q}_\mathsf{r} \cdot \bar{\mathbf{n}}_\mathcal{K}^\mathsf{r} & \forall \mathcal{S} \in \Gamma_{int}; \text{ and} \\
[\![v]\!] &:= v_\mathsf{l}\bar{\mathbf{n}}_\mathcal{K}^\mathsf{l} & [\![\mathbf{q}]\!] &:= \mathbf{q}_\mathsf{l} \cdot \bar{\mathbf{n}}_\mathcal{K}^\mathsf{l} & \forall \mathcal{S} \in \Gamma_{bou}
\end{aligned}
\tag{30}
$$

with $\bar{\mathbf{n}}_\mathcal{K}^\mathsf{l}$ and $\bar{\mathbf{n}}_\mathcal{K}^\mathsf{r}$ the spatial part of the unit space-time normal vectors $\mathbf{n}_\mathcal{K}^\mathsf{l} = (n_t^\mathsf{l}, \bar{\mathbf{n}}_\mathcal{K}^\mathsf{l})$ and $\mathbf{n}_\mathcal{K}^\mathsf{r} = (n_t^\mathsf{r}, \bar{\mathbf{n}}_\mathcal{K}^\mathsf{r})$ of the elements $\mathcal{K}_\mathsf{l}^n$ and $\mathcal{K}_\mathsf{r}^n$, respectively, at the face $\mathcal{S}$. Note that $\bar{\mathbf{n}}_\mathcal{K}^\mathsf{l} = -\bar{\mathbf{n}}_\mathcal{K}^\mathsf{r}$.

Now the following relation holds between jumps and averages:

$$
\sum_\mathcal{K} \int_{\partial \mathcal{K}_\mathsf{k}^n} v^-\,(\bar{\mathbf{n}}_\mathcal{K} \cdot \mathbf{q}^-)\, \mathrm{d}(\partial\mathcal{K}) = \int_\Gamma [\![v]\!] \cdot \{\!\{\mathbf{q}\}\!\}\, \mathrm{d}\mathcal{S} + \int_{\Gamma_{int}} \{\!\{v\}\!\}[\![\mathbf{q}]\!]\, \mathrm{d}\mathcal{S}.
\tag{31}
$$

Further, we can deduce the following properties of trace operators:

$$
\begin{aligned}
[\![f \pm g]\!] = [\![f]\!] \pm [\![g]\!], \quad \{\!\{f \pm g\}\!\} = \{\!\{f\}\!\} \pm \{\!\{g\}\!\}, \\
\{\!\{\{\!\{f\}\!\}\}\!\} = \{\!\{f\}\!\} \quad \text{and} \quad [\![\{\!\{f\}\!\}]\!] = 0
\end{aligned}
\tag{32}
$$

with $f, g \in V_\mathsf{h}$ or $\Sigma_\mathsf{h}$.

## 4.4 Global and local lifting operators

For the standard space-time discontinuous Galerkin formulation, we need to define the global lifting operator $\mathcal{R} : (L^2(\Gamma))^3 \to \Sigma_\mathsf{h}$ as

$$
\int_{\mathcal{E}_\mathsf{h}^n} \mathcal{R}(p) \cdot \tau\, \mathrm{d}\mathcal{K} := \int_\Gamma p \cdot \{\!\{\tau\}\!\}\, \mathrm{d}\mathcal{S}
\tag{33}
$$

and the local lifting operator $\mathcal{R}_\mathcal{S} : (L^2(\mathcal{S}))^3 \to \Sigma_\mathsf{h}$ as

$$
\int_{\mathcal{E}_\mathsf{h}^n} \mathcal{R}_\mathcal{S}(p) \cdot \tau\, \mathrm{d}\mathcal{K} := \int_\mathcal{S} p \cdot \{\!\{\tau\}\!\}\, \mathrm{d}\mathcal{S}.
\tag{34}
$$

Since $\Gamma = \bigcup \mathcal{S}$ is the union of all faces $\mathcal{S}$, we can relate the global and local lifting operators as

$$
\int_{\mathcal{E}_\mathsf{h}^n} \mathcal{R}(p) \cdot \tau\, \mathrm{d}\mathcal{K} = \sum_\mathcal{S} \int_\mathcal{S} p \cdot \{\!\{\tau\}\!\}\, \mathrm{d}\mathcal{S} = \sum_\mathcal{S} \int_{\mathcal{E}_\mathsf{h}^n} \mathcal{R}_\mathcal{S}(p) \cdot \tau\, \mathrm{d}\mathcal{K}.
\tag{35}
$$

The global and local lifting operator $\mathcal{R}(p)$ and $\mathcal{R}_\mathcal{S}(p)$ can be further split per space-time element $\mathcal{K}_\mathsf{k}^n$ as

$$
\int_{\mathcal{E}_\mathsf{h}^n} \mathcal{R}(p) \cdot \tau\, \mathrm{d}\mathcal{K} = \sum_\mathcal{K} \int_{\mathcal{K}_\mathsf{k}^n} \mathcal{R}_\mathsf{k}(p) \cdot \tau_\mathsf{k}\, \mathrm{d}\mathcal{K} \quad \text{and} \quad \int_{\mathcal{E}_\mathsf{h}^n} \mathcal{R}_\mathcal{S}(p) \cdot \tau\, \mathrm{d}\mathcal{K} = \sum_\mathcal{K} \int_{\mathcal{K}_\mathsf{k}^n} \mathcal{R}_{\mathcal{S},\mathsf{k}}(p) \cdot \tau_\mathsf{k}\, \mathrm{d}\mathcal{K}
\tag{36}
$$

with $\mathcal{R}_\mathsf{k}(p)$ the global lifting operator, $\mathcal{R}_{\mathcal{S},\mathsf{k}}(p)$ the local lifting operator and $\tau_\mathsf{k}$ the test function per space-time element $\mathcal{K}_\mathsf{k}^n$. Now using the arbitrariness of the test functions $\tau$, we can find that

the local lifting operator of a face $\mathcal{S}$ is non-zero only w.r.t the elements $\mathcal{K}_l^n$ and $\mathcal{K}_r^n$ connected to it because using (36) in (34), we get

$$\int_{\mathcal{K}_l^n} \mathcal{R}_{\mathcal{S},l}(p) \cdot \tau_l \, \mathrm{d}\mathcal{K} + \int_{\mathcal{K}_r^n} \mathcal{R}_{\mathcal{S},r}(p) \cdot \tau_r \, \mathrm{d}\mathcal{K} = \frac{1}{2} \int_{\mathcal{S}} p \cdot \tau_l \, \mathrm{d}\mathcal{S} + \frac{1}{2} \int_{\mathcal{S}} p \cdot \tau_r \, \mathrm{d}\mathcal{S}. \tag{37}$$

Moreover, we obtain the local lifting operators per space-time element $\mathcal{K}_k^n$ from (37) as

$$\int_{\mathcal{K}_k^n} \mathcal{R}_{\mathcal{S},k}(p) \cdot \tau_k = \int_{\mathcal{S}} \frac{1}{2} p \cdot \tau_k \, \mathrm{d}\mathcal{S} \quad \text{with } \mathcal{S} \subseteq \partial\mathcal{K}_k^n. \tag{38}$$

The global and local lifting operators can be further related per space-time element $\mathcal{K}_k^n$ using (36) and (37) in (35) as

$$\sum_{\mathcal{K}} \int_{\mathcal{K}_k^n} \mathcal{R}_k(p) \cdot \tau_k \, \mathrm{d}\mathcal{K} = \sum_{\mathcal{S}} \int_{\mathcal{E}_h^n} \mathcal{R}_{\mathcal{S}}(p) \cdot \tau \, \mathrm{d}\mathcal{K}$$

$$= \sum_{\mathcal{S}} \left( \int_{\mathcal{K}_l^n} \mathcal{R}_{\mathcal{S},l}(p) \cdot \tau_l \, \mathrm{d}\mathcal{K} + \int_{\mathcal{K}_r^n} \mathcal{R}_{\mathcal{S},r}(p) \cdot \tau_r \, \mathrm{d}\mathcal{K} \right)$$

$$= \sum_{\mathcal{K}} \int_{\mathcal{K}_k^n} \left( \sum_{\mathcal{S} \subset \partial\mathcal{K}_k^n} \mathcal{R}_{\mathcal{S},k}(p) \right) \cdot \tau_k \, \mathrm{d}\mathcal{K}, \tag{39}$$

and thus

$$\mathcal{R}_k(p) = \sum_{\mathcal{S} \subset \partial\mathcal{K}_k^n} \mathcal{R}_{\mathcal{S},k}(p). \tag{40}$$

## 4.5 Primal relation

To obtain the standard space-time DG formulation and the variational space-time DG formulation, we establish a relation between the approximations of velocity field $\mathbf{u}_h$ and the velocity potential $\phi_h$ using the primal formulation introduced by Arnold et al. [2] and Brezzi et al. [5]. For the primal formulation, we use the product rule

$$\bar{\nabla} \cdot (v\mathbf{q}) = \bar{\nabla} v \cdot \mathbf{q} + v(\bar{\nabla} \cdot \mathbf{q}), \tag{41}$$

with $v \in V_h$ and $\mathbf{q} \in \Sigma_h$, and the divergence theorem in space-time:

$$\int_{\mathcal{K}_k^n} \bar{\nabla} \cdot (v\mathbf{q}) \, \mathrm{d}\mathcal{K} = \int_{\mathcal{K}_k^n} \nabla \cdot (0, v\mathbf{q}) \, \mathrm{d}\mathcal{K} = \int_{\partial\mathcal{K}_k^n} \bar{\mathbf{n}}_{\mathcal{K}} \cdot (v^- \mathbf{q}^-) \, \mathrm{d}(\partial\mathcal{K}) \tag{42}$$

with $\nabla := (\partial_t, \partial_x, \partial_y, \partial_z)^T$.

To obtain the primal formulation, we discretize the auxiliary equation $\mathbf{u} = \bar{\nabla}\phi$ in (16) by multiplying it with arbitrary test functions $\tau_h \in \Sigma_h$ and introducing the approximations of the velocity and potential field $\mathbf{u}_h \in \Sigma_h$ and $\phi_h \in V_h$, respectively. Next, we integrate by parts over each space-time element $\mathcal{K}_k^n$ using (41), Gauss' divergence theorem in space-time and relation (31). We obtain after summation over all elements

$$\int_{\mathcal{E}_h^n} \mathbf{u}_h \cdot \tau_h \, \mathrm{d}\mathcal{K} = -\int_{\mathcal{E}_h^n} \phi_h(\bar{\nabla} \cdot \tau_h) \, \mathrm{d}\mathcal{K} + \int_{\Gamma} [\![\hat{\phi}]\!] \cdot \{\!\{\tau\}\!\} \, \mathrm{d}\mathcal{S} + \int_{\Gamma_{int}} \{\!\{\hat{\phi}\}\!\} [\![\tau]\!] \, \mathrm{d}\mathcal{S}. \tag{43}$$

In (43), we have introduced a numerical flux for the velocity potential $\hat{\phi} = \hat{\phi}(\phi_l, \phi_r)$ to take into account the multivalued traces $\phi_l$ and $\phi_r$ on each face $\mathcal{S} \in \Gamma$. The numerical flux $\hat{\phi}$ for elliptic problems (as suggested in Brezzi et al. [5]) is taken

$$\hat{\phi} := \{\!\{\phi_h\}\!\} \text{ on } \mathcal{S} \in \Gamma_{int} \text{ and } \hat{\phi} := \phi_h \text{ on } \mathcal{S} \in \Gamma_{bou}. \tag{44}$$

10

To obtain a primal relation between the velocity and potential field, we integrate (43) again by parts to get

$$\int_{\mathcal{E}_{h}^{n}} \mathbf{u}_{h} \cdot \tau_{h} d\mathcal{K} = \int_{\mathcal{E}_{h}^{n}} \bar{\nabla}\phi_{h} \cdot \tau_{h} d\mathcal{K} + \int_{\Gamma} [\![\hat{\phi} - \phi_{h}]\!] \cdot \{\!\{\tau\}\!\} d\mathcal{S} + \int_{\Gamma_{int}} \{\!\{\hat{\phi} - \phi_{h}\}\!\} [\![\tau]\!] d\mathcal{S}. \tag{45}$$

Now, we introduce the definition of global lifting operator (33) in (45), and use (44) to find

$$\int_{\mathcal{E}_{h}^{n}} \mathbf{u}_{h} \cdot \tau_{h} \, d\mathcal{K} = \int_{\mathcal{E}_{h}^{n}} \left( \bar{\nabla}\phi_{h} + \mathcal{R}([\![\hat{\phi} - \phi_{h}]\!]) \right) \cdot \tau_{h} \, d\mathcal{K}. \tag{46}$$

As test functions $\tau_{h}$ are arbitrary, the primal relation between $\mathbf{u}_{h}$ and $\phi_{h}$ becomes

$$\mathbf{u}_{h} = \bar{\nabla}\phi_{h} + \mathcal{R}([\![\hat{\phi} - \phi_{h}]\!]). \tag{47}$$

# 5 Standard space-time discontinuous Galerkin method

## 5.1 Weak formulation

The weak formulation of the velocity potential describing the free surface waves is obtained by multiplying the continuity equation $\bar{\nabla} \cdot \mathbf{u} = 0$ with arbitrary test functions $v \in V_{h}$, introducing the approximated velocity field $\mathbf{u}_{h} \in \Sigma_{h}$, integrating by parts and applying Gauss' divergence theorem (42) in space-time. Summing up over all elements and using relation (31), we obtain

$$\int_{\mathcal{E}_{h}^{n}} \mathbf{u}_{h} \cdot \bar{\nabla}v \, d\mathcal{K} = \int_{\Gamma} \hat{\mathbf{u}} \cdot [\![v]\!] \, d\mathcal{S}. \tag{48}$$

In the weak formulation (48), we have introduced a numerical flux $\hat{\mathbf{u}}$ for the velocity field as

$$\hat{\mathbf{u}} \cdot \bar{\mathbf{n}} := \begin{cases} \{\!\{\mathbf{u}_{h}\}\!\} \cdot \bar{\mathbf{n}} & \text{on } \Gamma_{int}, \\ g_{N} & \text{on } \Gamma_{L}, \\ 0 & \text{on } \Gamma_{B}, \\ \mathbf{u}_{h} \cdot \bar{\mathbf{n}} & \text{on } \Gamma_{S}. \end{cases} \tag{49}$$

Now, we eliminate the velocity field $\mathbf{u}_{h}$ from (48) using the primal relation (47) and by coupling the kinematic free surface boundary condition in (16) through the numerical flux (49) as

$$\hat{\mathbf{u}} \cdot \bar{\mathbf{n}} = \mathbf{u}_{h} \cdot \bar{\mathbf{n}} = \partial_{z}\phi_{h} = \partial_{t}\eta_{h}. \tag{50}$$

The weak formulation (48) now becomes

$$\int_{\mathcal{E}_{h}^{n}} \bar{\nabla}\phi_{h} \cdot \bar{\nabla}v \, d\mathcal{K} + \int_{\mathcal{E}_{h}^{n}} \mathcal{R}([\![\hat{\phi} - \phi_{h}]\!]) \cdot \bar{\nabla}v \, d\mathcal{K} = \int_{\Gamma_{int}} \{\!\{\bar{\nabla}\phi_{h}\}\!\} \cdot [\![v]\!] \, d\mathcal{S} +$$
$$\int_{\Gamma_{int}} \{\!\{\mathcal{R}([\![\hat{\phi} - \phi_{h}]\!])\}\!\} \cdot [\![v]\!] \, d\mathcal{S} + \int_{\Gamma_{L}} g_{N}v \, d\mathcal{S} + \int_{\Gamma_{S}} (\partial_{t}\eta_{h})v \, d\mathcal{S}. \tag{51}$$

For the space-time DG discretization, it is advantageous to expand and simplify the global lifting operator on the L.H.S. of (51) using (33) and (44) as

$$\int_{\mathcal{E}_{h}^{n}} \mathcal{R}([\![\hat{\phi} - \phi_{h}]\!]) \cdot \bar{\nabla}v \, d\mathcal{K} = - \int_{\Gamma_{int}} [\![\phi_{h}]\!] \cdot \{\!\{\bar{\nabla}v\}\!\} dS. \tag{52}$$

Also, the global lifting operator on the R.H.S. of (51) is approximated as

$$\{\!\{\mathcal{R}([\![\phi_{h}]\!])\}\!\} = \frac{1}{2} \left( \sum_{\mathcal{S} \subset \partial\mathcal{K}_{l}^{n}} \mathcal{R}_{\mathcal{S},l}([\![\phi_{h}]\!]) + \sum_{\mathcal{S} \subset \partial\mathcal{K}_{l}^{n}} \mathcal{R}_{\mathcal{S},r}([\![\phi_{h}]\!]) \right)$$
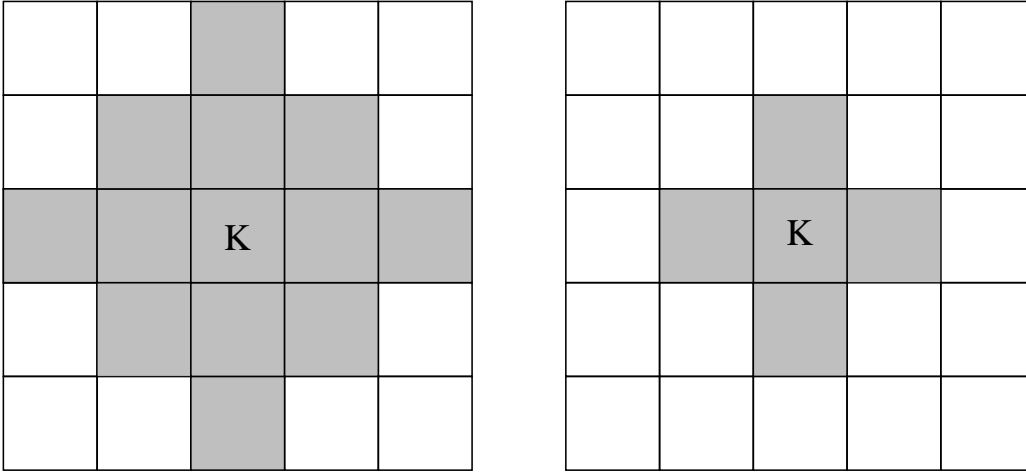
Figure 3: Sparsity of the global matrix w.r.t element K when using the global lifting operator $\mathcal{R}(\llbracket\phi\rrbracket)$ (left) and the approximate global lifting operator $n_{\mathcal{S}}\mathcal{R}_{\mathcal{S}}(\llbracket\phi\rrbracket)$ (right).

$$\approx n_{\mathcal{S}}\Big(\mathcal{R}_{\mathcal{S},\mathsf{l}}(\llbracket\phi_\mathsf{h}\rrbracket) + \mathcal{R}_{\mathcal{S},\mathsf{r}}(\llbracket\phi_\mathsf{h}\rrbracket)\Big) = n_{\mathcal{S}}\mathcal{R}_{\mathcal{S}}(\llbracket\phi_\mathsf{h}\rrbracket) \tag{53}$$

with $n_{\mathcal{S}}$ the number of faces of a space-time element. The approximation of the global lifting operator in (53) improves the sparsity of the global matrix resulting from the discretization of (51) as depicted in Fig. 3. Substituting (52) and (53) in (51), we obtain the simplified weak formulation

$$\int_{\mathcal{E}_\mathsf{h}^n} \bar\nabla\phi_\mathsf{h} \cdot \bar\nabla v \, \mathrm{d}\mathcal{K} = \int_{\Gamma_{int}} \llbracket\phi_\mathsf{h}\rrbracket \cdot \{\!\!\{\bar\nabla v\}\!\!\} \, \mathrm{d}\mathcal{S} + \int_{\Gamma_{int}} \{\!\!\{\bar\nabla\phi_\mathsf{h}\}\!\!\} \cdot \llbracket v\rrbracket \, \mathrm{d}\mathcal{S} -$$
$$\int_{\Gamma_{int}} n_{\mathcal{S}} \, \mathcal{R}_{\mathcal{S}}(\llbracket\phi_\mathsf{h}\rrbracket) \cdot \llbracket v\rrbracket \mathrm{d}\mathcal{S} + \int_{\Gamma_N} g_N v \mathrm{d}\mathcal{S} + \int_{\Gamma_S} \partial_t \eta_\mathsf{h} \mathrm{d}\mathcal{S}. \tag{54}$$

Now it remains to relate the free surface height to the velocity potential using the dynamic free surface boundary condition. Multiplying the dynamic free surface boundary condition in (16) with arbitrary test functions $w_\mathsf{h} \in W_\mathsf{h}$, introducing the approximations $\eta_\mathsf{h}$ and $\phi_\mathsf{h}$, and integrating over each face $\mathcal{S}$ of the free surface $\Gamma_S$, we obtain

$$\int_{\Gamma_S} (\partial_t \phi_\mathsf{h} + g\eta_\mathsf{h}) w_\mathsf{h} \mathrm{d}\mathcal{S} = 0. \tag{55}$$

The weak formulations (54) and (55) in the space-time slab $\mathcal{E}_\mathsf{h}^n$ are, however, not coupled to the previous space-time slab $\mathcal{E}_\mathsf{h}^{n-1}$.

To couple the space-time slabs, the last contribution in (54) is integrated by parts twice in time on each face $\mathcal{S} \in \Gamma_S$ of the free surface boundary, and after summing up over all free surfaces we obtain

$$\int_{\Gamma_S} (\partial_t \eta) v_\mathsf{h} \mathrm{d}\mathcal{S} = \int_{\Gamma_S} (\partial_t \eta) v_\mathsf{h} \mathrm{d}\mathcal{S} - \sum_{\mathcal{S}\in\Gamma_S} \int_{\partial\mathcal{S}} n_{\mathcal{S},t}(\hat\eta - \eta^-) v^- \mathrm{d}(\partial\mathcal{S}), \tag{56}$$

in which $n_{\mathcal{S},t}$ is the temporal component of the outward unit normal vector $\mathbf{n}_{\mathcal{S}}$ of the free surface boundary edge $\partial\mathcal{S}$ w.r.t. the free surface $\mathcal{S} \in \Gamma_S$, $\hat\eta$ is the numerical flux in time for the wave height $\eta$, and $\eta^- = \lim_{\epsilon\to 0} \eta_\mathsf{h}(t - \epsilon n_{\mathcal{S},t})$. We also treat the time derivatives on $\phi$ in (55) similarly, to obtain

$$\int_{\Gamma_S} (\partial_t \phi) w_\mathsf{h} \mathrm{d}\mathcal{S} = \int_{\Gamma_S} (\partial_t \phi) w_\mathsf{h} \mathrm{d}\mathcal{S} - \sum_{\mathcal{S}\in\Gamma_S} \int_{\partial\mathcal{S}} n_{\mathcal{S},t}(\hat\phi - \phi^-) w^- \mathrm{d}(\partial\mathcal{S}) \tag{57}$$

12

with $\hat{\phi}$ the numerical flux in time for the velocity potential $\phi$. The numerical fluxes $\hat{\eta}$ and $\hat{\phi}$ are defined as

$$\hat{\phi} := \begin{cases} \phi^+ & \text{on } \partial\mathcal{S}(t_{n-1}^-), \\ \phi^- & \text{on } \partial\mathcal{S}\backslash\partial\mathcal{S}(t_{n-1}^-), \end{cases} \quad \text{and } \hat{\eta} := \begin{cases} \eta^+ & \text{on } \partial\mathcal{S}(t_{n-1}^-), \\ \eta^- & \text{on } \partial\mathcal{S}\backslash\partial\mathcal{S}(t_{n-1}^-). \end{cases} \tag{58}$$

Finally, we introduce the bilinear form $B_{\mathsf{h}} : V_{\mathsf{h}} \times V_{\mathsf{h}} \mapsto \mathbb{R}$ as

$$B_{\mathsf{h}}(\phi_{\mathsf{h}}, v) := \int_{\mathcal{E}_{\mathsf{h}}^n} \bar{\nabla}\phi_{\mathsf{h}} \cdot \bar{\nabla}v \, \mathrm{d}\mathcal{K} - \int_{\Gamma_{int}} [\![\phi]\!] \cdot \{\!\{\bar{\nabla}v\}\!\} \, \mathrm{d}\mathcal{S} - \int_{\Gamma_{int}} \{\!\{\bar{\nabla}\phi_{\mathsf{h}}\}\!\} \cdot [\![v]\!] \, \mathrm{d}\mathcal{S}$$

$$+ \int_{\Gamma_{int}} n_{\mathcal{S}}\Big(\mathcal{R}_{\mathcal{S}}([\![\phi]\!]) \cdot [\![v]\!]\Big) \, \mathrm{d}\mathcal{S}, \tag{59}$$

the linear form $L_{\mathsf{h}} : V_{\mathsf{h}} \mapsto \mathbb{R}$ as

$$L_{\mathsf{h}}(v) := \int_{\Gamma_N} g_N v \, \mathrm{d}\mathcal{S}, \tag{60}$$

and substitute (56), (57) and (58) into (54) and (55). Hence, we can state the space-time discontinuous Galerkin weak formulation for linear free surface water waves as follows:
*Find a $\phi_{\mathsf{h}} \in V_{\mathsf{h}}$ and $\eta_{\mathsf{h}} \in W_{\mathsf{h}}$ such that for all $v_{\mathsf{h}} \in V_{\mathsf{h}}$ and $w_{\mathsf{h}} \in W_{\mathsf{h}}$*

$$B_{\mathsf{h}}(\phi_{\mathsf{h}}, v_{\mathsf{h}}) - \Big(\partial_t \eta_{\mathsf{h}}, v_{\mathsf{h}}\Big)_{\Gamma_S} - \Big(\eta^- - \eta^+, v^-\Big)_{\Gamma_S(t_{n-1}^-)} = L_{\mathsf{h}}(v_{\mathsf{h}})$$

$$\Big(\partial_t \phi_{\mathsf{h}}, w_{\mathsf{h}}\Big)_{\Gamma_S} + \Big(g\eta_{\mathsf{h}}, w_{\mathsf{h}}\Big)_{\Gamma_S} + \Big(\phi^- - \phi^+, w^-\Big)_{\Gamma_S(t_{n-1}^-)} = 0 \tag{61}$$

*is satisfied with $\Gamma_S(t_{n-1}^-) = \bigcup \partial\mathcal{S}(t_{n-1}^-)$ and $(u, v)_{\Gamma_S} := \int_{\Gamma_S} u \, v \, \mathrm{d}\mathcal{S}$.*

## 5.2 Space-time discontinuous Galerkin discretization

To obtain the space-time DG discretization, we first discretize the local lifting operator $\mathcal{R}_{\mathcal{S},\mathsf{k}}([\![\phi]\!])$ per space-time element $\mathcal{K}_{\mathsf{k}}^n$. This is done by expanding the local lifting operator $\mathcal{R}_{\mathcal{S},\mathsf{k}}([\![\phi]\!])$ as

$$(\mathcal{R}_{\mathcal{S},\mathsf{k}}([\![\phi]\!]))_k = \sum_{j=1}^{n_p} \hat{R}_{k,j}^{\mathcal{S},\mathsf{k}} \psi_{\mathsf{k},j} \tag{62}$$

and choosing the test function $\tau_{\mathsf{h}}$ in (38) as $\psi_{\mathsf{k},i}$, to get

$$\sum_{j=1}^{n_p} \hat{R}_{k,j}^{\mathcal{S},\mathsf{k}} \int_{\mathcal{K}_{\mathsf{k}}^n} \psi_{\mathsf{k},j}\psi_{\mathsf{k},i} \, \mathrm{d}\mathcal{K} = \frac{1}{2}\sum_{j=1}^{n_p} \Big(\hat{\phi}_{\mathsf{l},j} \int_{\mathcal{S}} n_k^{\mathsf{l}} \psi_{\mathsf{l},j}\psi_{\mathsf{k},i} \, \mathrm{d}\mathcal{S} + \hat{\phi}_{\mathsf{r},j} \int_{\mathcal{S}} n_k^{\mathsf{r}} \psi_{\mathsf{r},j}\psi_{\mathsf{k},i} \, \mathrm{d}\mathcal{S}\Big), \tag{63}$$

for each face $\mathcal{S} \in \Gamma_{int} \cap \partial\mathcal{K}_{\mathsf{k}}^n$, where the $\psi_{\mathsf{k},j}$'s are the basis functions and $\hat{R}_{k,j}^{\mathcal{S},\mathsf{k}}$'s the expansion coefficients for each component of $\mathcal{R}_{\mathcal{S},\mathsf{k}}([\![\phi]\!])_k$ with $k = 1, 2, 3$.

The space-time finite element discretization is obtained by substituting the polynomial expansions for the velocity potential $\phi_{\mathsf{h}}$, the free surface height $\eta_{\mathsf{h}}$ and the local lifting operator $\mathcal{R}_{\mathcal{S},\mathsf{k}}([\![\phi]\!])$ in space-time discontinuous Galerkin weak formulation (61), and choosing the test functions $v_{\mathsf{h}}$ and $w_{\mathsf{h}}$ as $\psi_{\mathsf{k},i}$ and $\varphi_i$, respectively. The resulting space-time finite element discretization for (61) is given in (100), (101) and (102), presented in Appendix A.1. Subsequently, we obtain a linear system of algebraic equations by eliminating $\hat{R}_{k,j}^{\mathcal{S},\mathsf{k}}$ and $\hat{\eta}_{\mathsf{l},j}^n$, using the relations (63) and (102) into (100) and (101), and combining them.

With the help of the notation (103) introduced in Appendix A.1, the expansion coefficients of local lifting operator $\mathcal{R}_{\mathcal{S},\mathsf{k}}$ for each face $\mathcal{S}$ can be expressed in terms of the expansion coefficients of the velocity potential $\phi_{\mathsf{h}}$, using (63), as

$$\hat{R}_k^{\mathcal{S},\mathsf{k}} = \frac{1}{2}(A^{\mathcal{K},\mathsf{k}})^{-1}\big(D_k^{\mathcal{S},\mathsf{lk}} \, \hat{\phi}_{\mathsf{l}} + D_k^{\mathcal{S},\mathsf{rk}} \, \hat{\phi}_{\mathsf{r}}\big). \tag{64}$$

13

Similarly, we can relate the expansion coefficients $\hat{\eta}_l^n$ and $\hat{\phi}_l^n$, using (102), as

$$\hat{\eta}_l^n = -[(H^{\mathcal{S}})^{-1}]_{n_q \times n_q}\Big([G^{\mathcal{S}}]_{n_q \times n_p}\hat{\phi}_l^n - [F^{\mathcal{S},\phi}]_{n_q \times 1}\Big). \tag{65}$$

Substituting (100) and (101) in the first equation of the (61), rearranging some terms, and eliminating $\hat{\eta}^n$ and $\hat{R}_k^{\mathcal{S},k}$ using the algebraic relations (64) and (65), we finally obtain the following linear algebraic system

$$\mathcal{L}\Phi^n = \mathcal{X} \tag{66}$$

with $\mathcal{L}$ the global matrix, $\Phi^n$ the unknown expansion coefficients of velocity potential and $\mathcal{X}$ the right hand side. The global matrix $\mathcal{L}$ in (66) is defined as

$$\mathcal{L} := \sum_{\mathcal{K}} B^{kk} + \sum_{\mathcal{S} \in \Gamma_S} [\bar{G}^{\mathcal{S}}]_{n_p \times n_q}[(H^{\mathcal{S}})^{-1}]_{n_q \times n_q}[G^{\mathcal{S}}]_{n_q \times n_p}$$

$$\sum_{\mathcal{S} \in \Gamma_{int}} -\frac{1}{2}\big(C^{\mathsf{ll},\mathcal{S}} + (C^{\mathsf{ll},\mathcal{S}})^T + \frac{n_{\mathcal{S}}}{4}M_{ij}^{ll} - \frac{1}{2}\big(C^{\mathsf{lr},\mathcal{S}} + (C^{\mathsf{rl},\mathcal{S}})^T + \frac{n_{\mathcal{S}}}{4}M_{ij}^{lr}$$

$$-\frac{1}{2}\big(C^{\mathsf{rl},\mathcal{S}} + (C^{\mathsf{lr},\mathcal{S}})^T + \frac{n_{\mathcal{S}}}{4}M_{ij}^{rl} - \frac{1}{2}\big(C^{\mathsf{rr},\mathcal{S}} + (C^{\mathsf{rr},\mathcal{S}})^T + \frac{n_{\mathcal{S}}}{4}M_{ij}^{rr}, \tag{67}$$

and the right hand side of (66) as

$$\mathcal{X} = \sum_{\mathcal{S} \in \Gamma_L} E^{\mathcal{S},l} + \sum_{\mathcal{S} \in \Gamma_S}(-F^{\mathcal{S},\eta} + [\bar{G}^{\mathcal{S}}]_{n_p \times n_q}[(H^{\mathcal{S}})^{-1}]_{n_q \times n_q}[F^{\mathcal{S},\phi}]_{n_q \times 1}); \tag{68}$$

for definitions of these new matrices on the respective right hand sides, see Appendix A.1. Given $\hat{\phi}^{n-1}$ and $\hat{\eta}^{n-1}$, we can construct the linear system $\mathcal{L}\Phi^n = \mathcal{X}$ and solve for $\Phi^n$. Subsequently, we obtain $\hat{\eta}^n$ using (65).

# 6 Space-time variational (dis)continuous Galerkin method

## 6.1 Variational formulation

For the discrete variational formulation of linear free surface waves, we introduce the horizontal cross section of the computational flow domain $\Omega_{\mathsf{h}}$ as $\bar{\Omega}_{\mathsf{h}}(z)$. Now, we define the total discrete kinetic energy $E_{K_{\mathsf{h}}}$ and the total discrete potential energy $E_{P_{\mathsf{h}}}$ in each space-time slab $\mathcal{E}_{\mathsf{h}}^n$ as

$$E_{K_{\mathsf{h}}} = \int_{\mathcal{E}_{\mathsf{h}}^n} \frac{1}{2}|\mathbf{u}_{\mathsf{h}}|^2 \, \mathrm{d}\mathcal{K} - \int_{\Gamma_L} g_N \phi_{\mathsf{h}} \, \mathrm{d}\mathcal{S} \quad \text{and} \quad E_{P_{\mathsf{h}}} = \int_{\Gamma_S} \frac{1}{2}g\eta_{\mathsf{h}}^2 \, \mathrm{d}\mathcal{S}, \tag{69}$$

where

$$\int_{\mathcal{E}_{\mathsf{h}}^n} \mathrm{d}\mathcal{K} = \int_{t_{n-1}}^{t_n} \int_{-H}^{0} \int_{\bar{\Omega}_{\mathsf{h}}} \mathrm{d}x\mathrm{d}y\mathrm{d}z\mathrm{d}t \quad \text{and} \quad \int_{\Gamma_S} \mathrm{d}\mathcal{S} = \int_{t_{n-1}}^{t_n} \int_{\bar{\Omega}_{\mathsf{h}}(z=0)} \mathrm{d}x\mathrm{d}y\mathrm{d}t.$$

In (69), we directly introduce the relation $\mathbf{u}_{\mathsf{h}} = \bar{\nabla}\phi_{\mathsf{h}} + \mathcal{R}([\![\hat{\phi} - \phi_{\mathsf{h}}]\!])$ obtained from the primal relation (47). The use of the global lifting operator, however, does not result into a discretization with a compact stencil. We therefore redefine the first term of the kinetic energy in (69) using local lifting operators as

$$E_{K_{\mathsf{h}}} = \int_{\mathcal{E}_{\mathsf{h}}^n} \frac{1}{2n_S}\Big(\sum_{\mathcal{S} \subset \partial \mathcal{K}_k^n}\big(\bar{\nabla}\phi_{\mathsf{h}} + n_S \mathcal{R}_{\mathcal{S},k}([\![\hat{\phi} - \phi_{\mathsf{h}}]\!])\big)^2\Big)\mathrm{d}\mathcal{K} - \int_{\Gamma_L} g_N \phi_{\mathsf{h}}\mathrm{d}\mathcal{S} \tag{70}$$

with $n_S$ the number of faces of each space-time element $\mathcal{K}_k^n$. The discrete kinetic energy (70) is further expanded as

$$E_{K_{\mathsf{h}}} = \int_{\mathcal{E}_{\mathsf{h}}^n} \frac{1}{2}|\bar{\nabla}\phi_{\mathsf{h}}|^2 \, \mathrm{d}\mathcal{K} + \int_{\mathcal{E}_{\mathsf{h}}^n} \sum_{\mathcal{S} \subset \partial \mathcal{K}_k^n}\big(\bar{\nabla}\phi_{\mathsf{h}} \cdot \mathcal{R}_{\mathcal{S},k}([\![\hat{\phi} - \phi_{\mathsf{h}}]\!])\big) \, \mathrm{d}\mathcal{K} +$$

14

$$\int_{\mathcal{E}_h^n} \frac{n_S}{2} \sum_{\mathcal{S} \subset \partial \mathcal{K}_k^n} |\mathcal{R}_{\mathcal{S},k}(\llbracket \hat{\phi} - \phi_h \rrbracket)|^2 \, d\mathcal{K} - \int_{\Gamma_L} g_N \phi_h \, d\mathcal{S}, \tag{71}$$

where $\int_{\Gamma_L} d\mathcal{S} = \int_{t_{n-1}}^{t_n} \int_{\partial \Omega_L} dl \, dz \, dt$ with $l$ the horizontal coordinate of the boundary $\partial \Omega_L$. Finally, we define the discrete functional for linear free surfaces as

$$\mathcal{L}_h(\phi_h, \phi_{h,s}, \eta_h) = \int_{\Gamma_S} \phi_{h,s}(\partial_t \eta_h) \, d\mathcal{S} - (E_{K_h} + E_{P_h}). \tag{72}$$

The discrete variational formulation for the linear free surface waves is now

$$\delta \mathcal{L}_h(\phi_h, \phi_{h,s}, \eta_h) = 0, \tag{73}$$

where $\phi_{h,s} = \phi_h(t, x, y, z = 0)$ is the approximated velocity potential evaluated at the mean free surface and $\delta \mathcal{L}_h$ is the variational derivative defined as

$$\delta \mathcal{L}_h = \lim_{\epsilon \to 0} \frac{1}{\epsilon} \Big( \mathcal{L}_h(\phi_h + \epsilon \delta \phi_h, \phi_{h,s} + \epsilon \delta \phi_{h,s}, \eta_h + \epsilon \delta \eta_h) - \mathcal{L}_h((\phi_h, \phi_{h,s}, \eta_h)) \Big) \tag{74}$$

with $\delta \phi_h$, $\delta \phi_{h,s}$ and $\delta \eta_h$ the arbitrary variations.

Evaluating variational principle (73), using (74) and the relation

$$\mathcal{R}_{\mathcal{S},k}(\llbracket \hat{\phi} - \phi_h + \epsilon(\delta \hat{\phi} - \delta \phi_h) \rrbracket) = \mathcal{R}_{\mathcal{S},k}(\llbracket \hat{\phi} - \phi_h \rrbracket) + \epsilon \mathcal{R}_{\mathcal{S},k}(\llbracket \delta \hat{\phi} - \delta \phi_h \rrbracket), \tag{75}$$

we find

$$\int_{\Gamma_S} \big( \phi_{h,s} \partial_t(\delta \eta_h) - g \eta_h \delta \eta_h + (\partial_t \eta_h) \delta \phi_{h,s} \big) d\mathcal{S} - \int_{\mathcal{E}_h^n} \bar{\nabla} \phi_h \cdot \bar{\nabla}(\delta \phi_h) \, d\mathcal{K}$$

$$- \int_{\mathcal{E}_h^n} \sum_{\mathcal{S} \subset \partial \mathcal{K}_k^n} \Big( \bar{\nabla} \phi_h \cdot \mathcal{R}_{\mathcal{S},k}(\llbracket \delta \hat{\phi} - \delta \phi_h \rrbracket) + \bar{\nabla}(\delta \phi_h) \cdot \mathcal{R}_{\mathcal{S},k}(\llbracket \hat{\phi} - \phi_h \rrbracket) \Big) \, d\mathcal{K}$$

$$- \int_{\mathcal{E}_h^n} \sum_{\mathcal{S} \subset \partial \mathcal{K}_k^n} n_S \Big( \mathcal{R}_{\mathcal{S},k}(\llbracket \hat{\phi} - \phi_h \rrbracket) \cdot \mathcal{R}_{\mathcal{S},k}(\llbracket \delta \hat{\phi} - \delta \phi_h \rrbracket) \Big) d\mathcal{K} + \int_{\Gamma_L} g_N \delta \phi_h \, d\mathcal{S} = 0. \tag{76}$$

From a computational point of view, the local lifting operators are easier to compute on the faces of an element rather than on the element itself. So, we first rearrange the sum over elements in (76) into a sum over faces and use the fact that the local lifting operators are only non-zero in the elements connected to the face $\mathcal{S}$, to obtain

$$\int_{\Gamma_S} \big( \phi_{h,s} \partial_t(\delta \eta_h) - g \eta_h \delta \eta_h + (\partial_t \eta_h) \delta \phi_{h,s} \big) d\mathcal{S} + \int_{\Gamma_L} g_N \delta \phi_h \, d\mathcal{S} - \int_{\mathcal{E}_h^n} \bar{\nabla} \phi_h \cdot \bar{\nabla}(\delta \phi_h) \, d\mathcal{K}$$

$$- \sum_{\mathcal{S} \in \Gamma_{int}} \Big( \int_{\mathcal{K}_l^n} \big( \bar{\nabla} \phi_h \cdot \mathcal{R}_{\mathcal{S},l}(\llbracket \delta \hat{\phi} - \delta \phi_h \rrbracket) + \bar{\nabla}(\delta \phi_h) \cdot \mathcal{R}_{\mathcal{S},l}(\llbracket \hat{\phi} - \phi_h \rrbracket) \big) \, d\mathcal{K}$$

$$+ \int_{\mathcal{K}_r^n} \big( \bar{\nabla} \phi_h \cdot \mathcal{R}_{\mathcal{S},r}(\llbracket \delta \hat{\phi} - \delta \phi_h \rrbracket) + \bar{\nabla}(\delta \phi_h) \cdot \mathcal{R}_{\mathcal{S},r}(\llbracket \hat{\phi} - \phi_h \rrbracket) \big) \, d\mathcal{K} \Big)$$

$$- \sum_{\mathcal{S} \in \Gamma_{int}} \Big( \int_{\mathcal{K}_l^n} n_S \big( \mathcal{R}_{\mathcal{S},l}(\llbracket \hat{\phi} - \phi_h \rrbracket) \cdot \mathcal{R}_{\mathcal{S},l}(\llbracket \delta \hat{\phi} - \delta \phi_h \rrbracket) \big) d\mathcal{K}$$

$$+ \int_{\mathcal{K}_r^n} n_S \big( \mathcal{R}_{\mathcal{S},r}(\llbracket \hat{\phi} - \phi_h \rrbracket) \cdot \mathcal{R}_{\mathcal{S},r}(\llbracket \delta \hat{\phi} - \delta \phi_h \rrbracket) \big) d\mathcal{K} \Big)$$

$$- \sum_{\mathcal{S} \in \Gamma_{bou}} \int_{\mathcal{K}_l^n} \Big( \bar{\nabla} \phi_h \cdot \mathcal{R}_{\mathcal{S},l}(\llbracket \delta \hat{\phi} - \delta \phi_h \rrbracket) + \bar{\nabla}(\delta \phi_h) \cdot \mathcal{R}_{\mathcal{S},l}(\llbracket \hat{\phi} - \phi_h \rrbracket) \Big) \, d\mathcal{K}$$

$$- \sum_{\mathcal{S} \in \Gamma_{bou}} \int_{\mathcal{K}_l^n} n_S \Big( \mathcal{R}_{\mathcal{S},l}(\llbracket \hat{\phi} - \phi_h \rrbracket) \cdot \mathcal{R}_{\mathcal{S},l}(\llbracket \delta \hat{\phi} - \delta \phi_h \rrbracket) \Big) d\mathcal{K} = 0. \tag{77}$$

15

In (77), we define the numerical flux on the variations $\delta\phi_h$ as

$$\delta\hat{\phi} := \{\!\{\delta\phi_h\}\!\} \text{ on } \mathcal{S} \in \Gamma_{int} \quad \text{and} \quad \delta\hat{\phi} := \delta\phi_h \text{ on } \mathcal{S} \in \Gamma_{bou}, \tag{78}$$

which follows from the definition of the numerical flux for $\phi_h$ in (44). By using the definitions (44) and (78), and the properties in (32), we can deduce the following relations

$$[\![\hat{\phi} - \phi_h]\!] = -[\![\phi_h]\!] \text{ on } \mathcal{S} \in \Gamma_{int}, \qquad\qquad [\![\hat{\phi} - \phi_h]\!] = 0 \text{ on } \mathcal{S} \in \Gamma_{bou},$$

$$[\![\delta\hat{\phi} - \delta\phi_h]\!] = -[\![\delta\phi_h]\!] \text{ on } \mathcal{S} \in \Gamma_{int} \quad \text{and} \qquad [\![\delta\hat{\phi} - \delta\phi_h]\!] = 0 \text{ on } \mathcal{S} \in \Gamma_{bou}. \tag{79}$$

We now simplify (77) using (79) to obtain

$$\int_{\Gamma_S} \left( \phi_{h,s} \partial_t(\delta\eta_h) - g\eta_h\delta\eta_h + (\partial_t\eta_h)\delta\phi_{h,s} \right) \mathrm{d}\mathcal{S} + \int_{\Gamma_L} g_N \delta\phi_h \, \mathrm{d}\mathcal{S} - \int_{\mathcal{E}_h^n} \bar{\nabla}\phi_h \cdot \bar{\nabla}(\delta\phi_h) \, \mathrm{d}\mathcal{K}$$

$$+ \sum_{\mathcal{S} \in \Gamma_{int}} \left( \int_{\mathcal{K}_l^n} \left( \bar{\nabla}\phi_h \cdot \mathcal{R}_{\mathcal{S},l}([\![\delta\phi_h]\!]) + \bar{\nabla}(\delta\phi_h) \cdot \mathcal{R}_{\mathcal{S},l}([\![\phi_h]\!]) \right) \mathrm{d}\mathcal{K} \right.$$

$$+ \left. \int_{\mathcal{K}_r^n} \left( \bar{\nabla}\phi_h \cdot \mathcal{R}_{\mathcal{S},r}([\![\delta\phi_h]\!]) + \bar{\nabla}(\delta\phi_h) \cdot \mathcal{R}_{\mathcal{S},r}([\![\phi_h]\!]) \right) \mathrm{d}\mathcal{K} \right)$$

$$- \sum_{\mathcal{S} \in \Gamma_{int}} \left( \int_{\mathcal{K}_l^n} n_S \left( \mathcal{R}_{\mathcal{S},l}([\![\phi_h]\!]) \cdot \mathcal{R}_{\mathcal{S},l}([\![\delta\phi_h]\!]) \right) \mathrm{d}\mathcal{K} + \int_{\mathcal{K}_r^n} n_S \left( \mathcal{R}_{\mathcal{S},r}([\![\phi_h]\!]) \cdot \mathcal{R}_{\mathcal{S},r}([\![\delta\phi_h]\!]) \right) \mathrm{d}\mathcal{K} \right) = 0. \tag{80}$$

Finally, using definitions (29) and (34) and the arbitrariness of variations, we obtain the discrete variational formulation of the linear free surface waves as
*Find a $\bar{\phi}_h^n \in \bar{V}_h$ and $\bar{\eta}_h^n \in \bar{W}_h$ such that for all $\delta\bar{\phi}_h^n \in \bar{V}_h$ and $\delta\bar{\eta}_h^n \in \bar{W}_h$, equations*

$$\int_{\mathcal{E}_h^n} \bar{\nabla}\phi_h \cdot \bar{\nabla}(\delta\phi_h) \, \mathrm{d}\mathcal{K} - \sum_{\mathcal{S} \in \Gamma_{int}} \int_{\mathcal{S}} \left( \{\!\{\bar{\nabla}\phi_h\}\!\} \cdot [\![\delta\phi_h]\!] + \{\!\{\bar{\nabla}(\delta\phi_h)\}\!\} \cdot [\![\phi_h]\!] - \right.$$

$$\left. n_S \{\!\{\mathcal{R}_{\mathcal{S}}([\![\phi_h]\!])\}\!\} \cdot [\![\delta\phi_h]\!] \right) \mathrm{d}\mathcal{S} - \int_{\Gamma_L} g_N \delta\phi_h \, \mathrm{d}\mathcal{S} - \int_{\Gamma_S} (\partial_t\eta_h)\delta\phi_{h,s} \, \mathrm{d}\mathcal{S} = 0 \tag{81}$$

*and*

$$\int_{\Gamma_S} \left( \phi_{h,s}\partial_t(\delta\eta_h) - g\eta_h\delta\eta_h \right) \mathrm{d}\mathcal{S} = 0 \tag{82}$$

*are satisfied with end point conditions $\delta\phi_h(t_{n-1}) = \delta\eta_h(t_{n-1}) = \delta\phi_h(t_n) = \delta\eta_h(t_n) = 0$, where the approximations $\phi_h$ and $\eta_h$ are defined as in (27).* To satisfy these end point conditions on the variations, we define the expansions of variations

$$\delta\phi_h = \psi^n \psi^{n-1} \delta\bar{\phi}_h^n \quad \text{and} \quad \delta\bar{\eta}_h = \psi^n \psi^{n-1} \delta\bar{\eta}_h^n \tag{83}$$

such that they vanish at $t_n$ and $t_{n-1}$ but are non-zero within the space-time element. These are coupled with the previous space-time domain $\mathcal{E}_h^{n-1}$ by imposing the continuity in time. While the variables are a piecewise continuous linear approximation in time between the two time levels, the variations are forced to be zero at the end points and are thus defined differently. The basis and test functions are therefore unequal. For the harmonic oscillator, such a choice of continuous approximation for variables and vanishing test functions at the end points in each time interval led to the energy-conserving modified mid-point scheme, derived in §2.

## 6.2 Variational finite element discretization

To obtain the variational finite element discretization, we first have to discretize the local lifting operators $\mathcal{R}_{\mathcal{S},k}([\![\phi_h]\!])$ per space-time element $\mathcal{K}_k^n$. Using a similar approximation as given in (27) for $\phi_h$, the local lifting operator $\mathcal{R}_{\mathcal{S},k}([\![\phi_h]\!])$ is expanded as

$$\mathcal{R}_{\mathcal{S},k}([\![\phi_h]\!]) = \bar{\mathcal{R}}_{\mathcal{S},k}^n([\![\phi_h]\!])\psi^n + \bar{\mathcal{R}}_{\mathcal{S},k}^{n-1}([\![\phi_h]\!])\psi^{n-1}. \tag{84}$$

16

with $\bar{\mathcal{R}}_{\mathcal{S},\mathsf{k}}^n(\llbracket\phi_\mathsf{h}\rrbracket)$ the local lifting operator on the spatial element $K_\mathsf{k}^n$. Thereafter, we define the expansion of the local lifting operator $\bar{\mathcal{R}}_{\mathcal{S},\mathsf{k}}^n(\llbracket\phi_\mathsf{h}\rrbracket)$ akin to (62) as

$$(\bar{\mathcal{R}}_{\mathcal{S},\mathsf{k}}^n(\llbracket\phi_\mathsf{h}\rrbracket))_k = \sum_{j=1}^{n_p} \hat{R}_{k,j}^{\mathcal{S},kn} \bar{\psi}_{\mathsf{k},j} \tag{85}$$

with $\hat{R}_{k,j}^{\mathcal{S},kn}$ the expansion coefficients for each component of $\bar{\mathcal{R}}_{\mathcal{S},\mathsf{k}}^n(\llbracket\phi_\mathsf{h}\rrbracket)_k$ with $k = 1, 2, 3$. The discretization of the local lifting operator $\bar{\mathcal{R}}_{\mathcal{S},\mathsf{k}}^n(\llbracket\phi_\mathsf{h}\rrbracket)$ arises from (38) as

$$\sum_{j=1}^{n_p} \hat{R}_{k,j}^{\mathcal{S},kn} \int_{\mathcal{K}_\mathsf{k}^n} \bar{\psi}_{\mathsf{k},j}\bar{\psi}_{\mathsf{k},i} \, \mathrm{d}K = \frac{1}{2}\sum_{j=1}^{n_p} \left( \hat{\phi}_{\mathsf{l},j}^n \int_{\mathcal{S}} \bar{n}_k^\mathsf{l}\bar{\psi}_{\mathsf{l},j}\bar{\psi}_{\mathsf{k},i} \, \mathrm{d}\mathcal{S} + \hat{\phi}_{\mathsf{r},j}^n \int_{\mathcal{S}} \bar{n}_k^\mathsf{r}\bar{\psi}_{\mathsf{r},j}\bar{\psi}_{\mathsf{k},i} \, \mathrm{d}\mathcal{S} \right) \tag{86}$$

for $\mathcal{S} \in \Gamma_{int} \cap \partial\mathcal{K}_\mathsf{k}^n$ with $\bar{\psi}_{\mathsf{k},j}$ the basis function.

The space-time variational finite element discretization can now be obtained by substituting the polynomial expansion for the velocity potential $\phi_\mathsf{h}$, the free surface height $\eta_\mathsf{h}$ and the local lifting operator $\mathcal{R}_{\mathcal{S},\mathsf{k}}(\llbracket\phi\rrbracket)$ in the variational formulation (81) and (82), and using the arbitrariness of the variations $\delta\hat{\phi}_\mathsf{h}^n$, $\delta\bar{\phi}_{s,\mathsf{h}}$ and $\delta\bar{\eta}_\mathsf{h}$. The variations $\delta\phi_\mathsf{h}$ are varied as $\psi^n\psi^{n-1}\bar{\psi}_{\mathsf{k},i}$ for $i = 1, \ldots, n_p$, and $\delta\eta_\mathsf{h}$ as $\psi^n\psi^{n-1}\bar{\varphi}_{\mathsf{l},i}$ for $i = 1, \ldots, n_q$ such that they vanish at $t_n$ and $t_{n-1}$. Further, to simplify the finite element discretization we use the fact that the basis functions $\psi^n$ and $\psi^{n-1}$ are independent of space, the basis functions $\bar{\psi}_{\mathsf{k},i}$ and $\bar{\varphi}_{\mathsf{l},i}$ are independent of time, and the spatial element $K_\mathsf{k}$ does not deform in time to get the following simplifications:

$$\partial_t \bar{\psi}_{\mathsf{k},i} = 0, \quad \partial_t \bar{\varphi}_{\mathsf{l},i} = 0, \quad \bar{\nabla}\psi^n = 0 \quad \text{and} \quad \bar{\nabla}\psi^{n-1} = 0. \tag{87}$$

The resulting finite element discretization for the variational formulation (81) and (82) are given in (104) and (105), which are presented in the Appendix A.2. Subsequently, we obtain a linear system of algebraic equations by eliminating $\hat{R}_{k,j}^{\mathcal{S},kn}$ $\hat{\eta}_{\mathsf{l},j}^n$ using the relations (86) and (105) into (104).

With the help of the notations (106) introduced in Appendix A.2, the expansion coefficients of local lifting opertor $\mathcal{R}_{\mathcal{S},\mathsf{k}}^n$ for each face $\mathcal{S}$ can be expressed in terms of the expansion coefficients of the velocity potential $\phi_\mathsf{h}^n$ using (85) as

$$\hat{R}_k^{\mathcal{S},kn} = \frac{1}{2}(A^{\mathcal{K},\mathsf{k}})^{-1}\left(\hat{D}_k^{\mathcal{S},\mathsf{lk}} \, \hat{\phi}_\mathsf{l}^n + \hat{D}_k^{\mathcal{S},\mathsf{rk}} \, \hat{\phi}_\mathsf{r}^n\right). \tag{88}$$

Similarly, we can relate the expansion coefficients $\hat{\eta}_\mathsf{l}^n$ and $\hat{\phi}_\mathsf{l}^n$ using (105) with (106) as

$$\hat{\eta}_\mathsf{l}^n = (H^{\mathcal{S}})^{-1}\left(L^{\mathcal{S}}\hat{\phi}_\mathsf{l}^n + \bar{L}^{\mathcal{S}}\hat{\phi}_\mathsf{l}^{n-1} - \bar{H}^{\mathcal{S}}\hat{\eta}_\mathsf{l}^{n-1}\right). \tag{89}$$

Eliminating $\hat{\eta}^n$, $\hat{R}_k^{\mathcal{S},kn}$ and $\hat{R}_k^{\mathcal{S},k(n-1)}$ from (104) using (89) and (88), we obtain the following linear algebraic system

$$\mathcal{L}\Phi^n = \mathcal{X} \tag{90}$$

with $\mathcal{L}$ the global matrix, $\Phi^n$ the unknown expansion coefficients of the velocity potential, and $\mathcal{X}$ the right hand side. The global matrix $\mathcal{L}$ is defined as

$$\mathcal{L} = \sum_{\mathcal{K}} B^{kk} - \sum_{\mathcal{S}\in\Gamma_S} G^{\mathcal{S}}(H^{\mathcal{S}})^{-1}L^{\mathcal{S}} \sum_{\mathcal{S}\in\Gamma_{int}} -\frac{1}{2}\left(C^{\mathsf{ll},\mathcal{S}} + (C^{\mathsf{ll},\mathcal{S}})^T\right) + \frac{n_\mathcal{S}}{4}M_{ij}^{ll} - \frac{1}{2}\left(C^{\mathsf{lr},\mathcal{S}} + (C^{\mathsf{rl},\mathcal{S}})^T\right) + \frac{n_\mathcal{S}}{4}M_{ij}^{lr}$$

$$-\frac{1}{2}\left(C^{\mathsf{rl},\mathcal{S}} + (C^{\mathsf{lr},\mathcal{S}})^T\right) + \frac{n_\mathcal{S}}{4}M_{ij}^{rl} - \frac{1}{2}\left(C^{\mathsf{rr},\mathcal{S}} + (C^{\mathsf{rr},\mathcal{S}})^T\right) + \frac{n_\mathcal{S}}{4}M_{ij}^{rr}, \tag{91}$$

and the right hand side $\mathcal{X}$ in (90) as

$$\mathcal{X} = -\sum_{\mathcal{K}} \bar{B}^{kk}\hat{\phi}_\mathsf{k}^{n-1} + \sum_{\mathcal{S}\in\Gamma_L} E^{\mathcal{S},\mathsf{l}}$$

$$+ \sum_{\mathcal{S} \in \Gamma_S} G^{\mathcal{S}}(H^{\mathcal{S}})^{-1} \bar{L}^{\mathcal{S}} \hat{\phi}_{\mathsf{l}}^{n-1} + \left( \bar{G}^{\mathcal{S}} - G^{\mathcal{S}}(H^{\mathcal{S}})^{-1} \bar{H}^{\mathcal{S}} \right) \hat{\eta}_{\mathsf{l}}^{n-1}$$

$$+ \sum_{\mathcal{S} \in \Gamma_{int}} \left( \frac{1}{2} (\bar{C}^{\mathsf{ll},\mathcal{S}} + \bar{C}^{\mathsf{ll},\mathcal{S}})^T ) - \frac{n_{\mathcal{S}}}{4} \bar{M}_{ij}^{ll} \right) \hat{\phi}_{\mathsf{l}}^{n-1} + \left( \frac{1}{2} (\bar{C}^{\mathsf{lr},\mathcal{S}} + (\bar{C}^{\mathsf{rl},\mathcal{S}})^T ) - \frac{n_{\mathcal{S}}}{4} \bar{M}_{ij}^{lr} \right) \hat{\phi}_{\mathsf{r}}^{n-1} +$$

$$\left( \frac{1}{2} (\bar{C}^{\mathsf{rl},\mathcal{S}} + (\bar{C}^{\mathsf{lr},\mathcal{S}})^T ) - \frac{n_{\mathcal{S}}}{4} \bar{M}_{ij}^{rl} \right) \hat{\phi}_{\mathsf{l}}^{n-1} + \left( \frac{1}{2} (\bar{C}^{\mathsf{rr},\mathcal{S}} + (\bar{C}^{\mathsf{rr},\mathcal{S}})^T ) - \frac{n_{\mathcal{S}}}{4} \bar{M}_{ij}^{rr} \right) \hat{\phi}_{\mathsf{r}}^{n-1}. \tag{92}$$

Given $\phi_{\mathsf{h}}^{n-1}$ and $\eta_{\mathsf{h}}^{n-1}$, we can construct the linear system $\mathcal{L} \Phi^n = \mathcal{X}$ and solve it for $\phi_{\mathsf{h}}^n$. Subsequently, we obtain $\eta_{\mathsf{h}}^n$ using (89).

## 6.3   Solving the linear systems (66) and (90)

The global matrix $\mathcal{L}$ of the linear algebraic system has size $N_e n_p \times N_e n_p$, where $N_e$ is the number of elements in the computational domain $\mathcal{E}_{\mathsf{h}}^n$ and $n_p$ the number of degrees of freedom per element. It can be divided into $N_e \times N_e$ blocks with size $n_p \times n_p$. Further, the number of non-zero block rows in the global matrix $\mathcal{L}$ w.r.t each space-time element $\mathcal{K}_{\mathsf{k}}^n$ is directly dependent on its immediate neighbouring elements connected through the boundary of $\partial \mathcal{K}_{\mathsf{k}}^n$. Therefore, the global matrix $\mathcal{L}$ is of block sparse type with a compact stencil. Hence, we use a well-tested software tool kit called PETSc (see [20, 21, 22]) for building and solving the linear system.

This tool kit PETSc, a "Portable, Extensible Toolkit for Scientific Computation", consists of a number of sparse matrix storage routines and both iterative and direct sparse linear solvers. In particular, we use a sequential block sparse matrix storage routine for building the global matrix $\mathcal{L}$ and a linear solver based on a biconjugate gradient method with ILU preconditioner for solving the linear system $\mathcal{L} \Phi^n = \mathcal{X}$ (see the manual by Satish et al. [20]). For building the matrices, PETSc offers a preallocated matrix storage routine for which we have to specify the number of non-zero blocks in each row of the matrix. We have thus observed a tremendous increase of performance.

# 7   Numerical results

In this section, we present the numerical results obtained using the standard space-time DG and the variational space-time (dis)continuous Galerkin finite element schemes, and compare the numerical results with two exact solutions of the linear wave equations. The numerical implementation is done for the equations in non-dimensional form. We used the following scaling:

$$(x, y, z) \mapsto H \, (x, y, z), \quad t \mapsto \sqrt{\frac{H}{g}} \, t, \quad \phi \mapsto H \sqrt{gH} \, \phi \text{ and } \eta \mapsto H \, \eta. \tag{93}$$

We compute the $L^2(\Omega_{\mathsf{h}})$–norms of the errors in the numerical results for the velocity potential and free surface height as

$$\| \phi - \phi_{\mathsf{h}} \|_{L^2(\Omega_{\mathsf{h}})} := \left( \sum_{\mathcal{K}} \int_{\mathcal{K}_{\mathsf{k}}^n} (\phi - \phi_{\mathsf{h}})^2 \, \mathrm{d}\mathcal{K} \right)^{1/2} \text{ and} \tag{94}$$

$$\| \eta - \eta_{\mathsf{h}} \|_{L^2(\Gamma_S(t_n^-))} := \left( \sum_{\mathcal{S} \in \Gamma_S} \int_{\partial \mathcal{S}(t_n^-)} (\eta - \eta_{\mathsf{h}})^2 \, \mathrm{d}(\partial \mathcal{S}) \right)^{1/2}, \tag{95}$$

where $(\phi, \eta)$ and $(\phi_{\mathsf{h}}, \eta_{\mathsf{h}})$ are the exact and numerical solutions of the velocity potential and free surface wave height, respectively. The order of accuracy of the numerical scheme can be determined using

$$\mathsf{order} = \left( \ln(\mathsf{Error}^{(1)}) - \ln(\mathsf{Error}^{(2)}) \right) / \left( \ln(\mathsf{h}_{\mathcal{K}}^{(1)}) - \ln(\mathsf{h}_{\mathcal{K}}^{(2)}) \right), \tag{96}$$

18

where $\mathsf{Error}^{(1)}$ and $\mathsf{Error}^{(2)}$ are the errors computed on the meshes with cell measures $\mathsf{h}_{\mathcal{K}}^{(1)}$ and $\mathsf{h}_{\mathcal{K}}^{(2)}$, respectively. For all wave simulations, the computational grid size in the $z$-direction is chosen such that it decreases as we move from the free surface at $z = 0$ down to the bottom topography. This is in line with the harmonic solution in which the amplitude decreases exponentially going down from the rest level at $z = 0$.

## 7.1  Harmonic waves

The governing equations for the linear free surface waves in (16) satisfy the harmonic wave modes

$$\phi(x, y, z, t) = A_{l,m} \cos(k_x x + k_y y + \omega t) \cosh(k_z(z + H)) \tag{97}$$

on $\Omega = [0, 1]^2 \times [-H, 0]$, where $A_{l,m}$ is the amplitude; $H$ the mean water depth; $k_x = 2\pi l$, $k_y = 2\pi m$, and $k_z = \pm\sqrt{k_x^2 + k_y^2}$ are the wave numbers; $l$ and $m$ are integers; $\omega$ the frequency, and the dispersion relation is $\omega^2 = k_z \tanh(k_z H)$. The free surface evolution of the harmonic wave modes is obtained by using the kinematic free surface boundary condition $\partial_t \phi = g\eta$, as

$$\eta(x, y, t) = -A_{l,m}\omega \sin(k_x x + k_y y + \omega t) \cosh(k_z H) \text{ at } z = 0. \tag{98}$$

In both the space-time DG and space-time variational schemes, we initialize two harmonic modes with mean water depth $H = 1$, $(l, m) = (1, 1)$ and $(1, -1)$, and amplitudes $A_{1,1} = 2.32 \cdot 10^{-4}$ and $A_{1,-1} = 1.12 \cdot 10^{-4}$. The two modes have a time period $T = 2.1078$ and travel in diagonally opposite directions. The projections of the initial condition for the velocity potential and the free surface wave height are shown in Figs. 4(a) and (b).



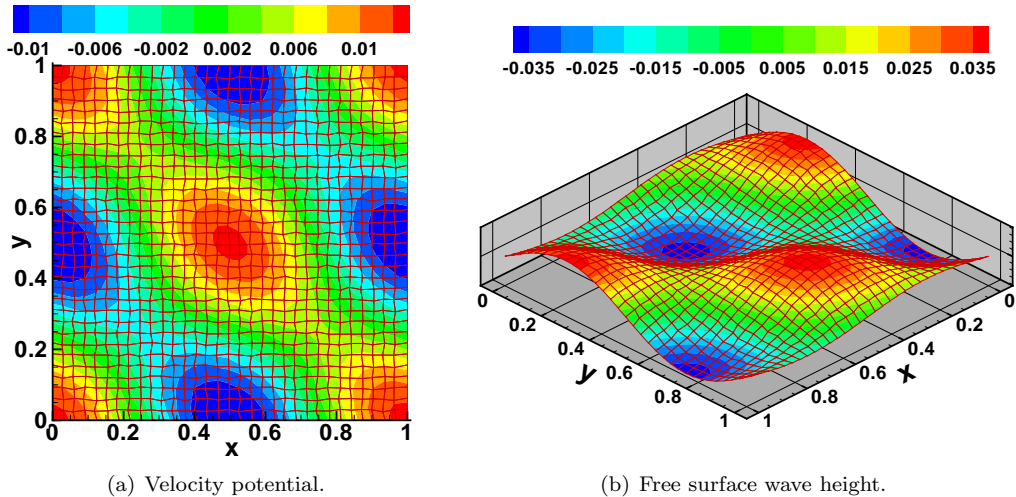(a) Velocity potential.  (b) Free surface wave height.

Figure 4: Contour plots of the velocity potential and the free surface wave height at time $t = 0$ on an irregular grid of size $32 \times 32 \times 8$.

To test the accuracy of the space-time discontinuous Galerkin and space-time variational schemes, we simulated these harmonic waves for one time period $T$ on various grids of sizes $8 \times 8 \times 2$, $16 \times 16 \times 2$, $32 \times 32 \times 4$ and $64 \times 64 \times 8$ with time steps $\Delta t = T/10$, $T/20$, $T/40$ and $T/80$, respectively. We also compute the errors of the velocity potential and free surface wave height in the $L^2$–norm and subsequently, determine the order of accuracy, presented in Tables 1 and 2. Both schemes are higher order accurate. Contour plots of the velocity potential and free surface wave height of the numerical simulations from both schemes are presented in Figs. 5 and 6. To qualitatively show the dispersion error and dissipation error of the space-time DG scheme and space-time variational scheme, we have

19

simulated the harmonic waves for about 10 time periods. We observe from the Figs. 7(a)-(j) that amplitude of the waves decays strongly when simulated with the space-time DG scheme whereas it does not decay with the space-time variational scheme, as expected.

Table 1: $L^2$–errors of the velocity potential and the free surface height at $t = T$ on a regular grid using (space-time DG scheme).

| Grid | | Velocity potential | | Free surface height | |
| --- | --- | --- | --- | --- | --- |
| $N_x \times N_y \times N_z$ | h | $L^2$–error | order | $L^2$–error | order |
| $8 \times 8 \times 2$ | 0.785155 | $9.0079 \cdot 10^{-04}$ | – | $5.2950 \cdot 10^{-03}$ | – |
| $16 \times 16 \times 4$ | 0.465848 | $1.9761 \cdot 10^{-04}$ | 2.85 | $1.4053 \cdot 10^{-03}$ | 2.54 |
| $32 \times 32 \times 8$ | 0.252864 | $4.9046 \cdot 10^{-05}$ | 2.29 | $3.5070 \cdot 10^{-04}$ | 2.27 |
| $64 \times 64 \times 16$ | 0.131652 | $1.1961 \cdot 10^{-05}$ | 2.17 | $8.7284 \cdot 10^{-05}$ | 2.13 |

Table 2: $L^2$–errors of the velocity potential and the free surface height at $t = T$ on a regular grid (variational space-time DG scheme) with $p^{\text{th}}$–order polynomial approximation.

| Grid | Cell size | Velocity potential | | Free surface height | |
| --- | --- | --- | --- | --- | --- |
| $N_x \times N_y \times N_z$ | h | $L^2$–error | order | $L^2$–error | order |
| For $p = 1$ | | | | | |
| $8 \times 8 \times 2$ | 0.785155 | $1.8445 \cdot 10^{-03}$ | – | $2.3505 \cdot 10^{-02}$ | – |
| $16 \times 16 \times 4$ | 0.465848 | $6.1255 \cdot 10^{-04}$ | 2.11 | $8.2809 \cdot 10^{-03}$ | 2.00 |
| $32 \times 32 \times 8$ | 0.252864 | $1.9072 \cdot 10^{-04}$ | 1.91 | $2.4410 \cdot 10^{-03}$ | 2.00 |
| $64 \times 64 \times 16$ | 0.131652 | $4.9538 \cdot 10^{-05}$ | 2.07 | $6.3329 \cdot 10^{-04}$ | 2.07 |
| For $p = 2$ | | | | | |
| $8 \times 8 \times 2$ | 0.785155 | $1.6963 \cdot 10^{-03}$ | – | $1.0409 \cdot 10^{-04}$ | – |
| $16 \times 16 \times 4$ | 0.465848 | $2.4237 \cdot 10^{-05}$ | 2.79 | $1.8443 \cdot 10^{-04}$ | 4.25 |
| $32 \times 32 \times 8$ | 0.252864 | $2.7994 \cdot 10^{-06}$ | 3.53 | $1.6339 \cdot 10^{-05}$ | 3.97 |

## 7.2 Linear waves generated by a wave maker

Consider a wave basin $\Omega = [0,1]^2 \times [-H, 0]$ with solid walls on all sides except a piston type wave maker on the side at $x = 1$. Given the normal velocity of the wave maker as $g_N = -Ak_x \cos(\omega t) \cos(k_y y) \cosh(k_z(z + H))$, we derive an exact solution for the velocity potential and free surface height as

$$\phi(t, x, y, z) = A \cos(\omega t) \ \cos(k_x x) \cos(k_y y) \cosh(k_z(z + H)) \quad \text{and}$$
$$\eta(t, x, y) = -A\omega \sin(\omega t) \ \cos(k_x x) \cos(k_y y) \cosh(k_z H) \tag{99}$$

with $A$ the wave amplitude, $H$ the mean water depth, $k_x = (2l + 1)\pi/2$, $k_y = 2m\pi$, $k_z^2 = (k_x^2 + k_y^2)$, $\omega$ the frequency satisfying the dispersion relation $\omega^2 = k_z \tanh(k_z H)$; and, $l$ and $m$ are integers.

To simulate the waves generated by a wave maker, we initialize the flow field $(\eta, \phi)$ with the exact solution, prescribe the normal velocity of the wave maker at the boundary $x = 1$ and take the

(a) At $t = T/2$.
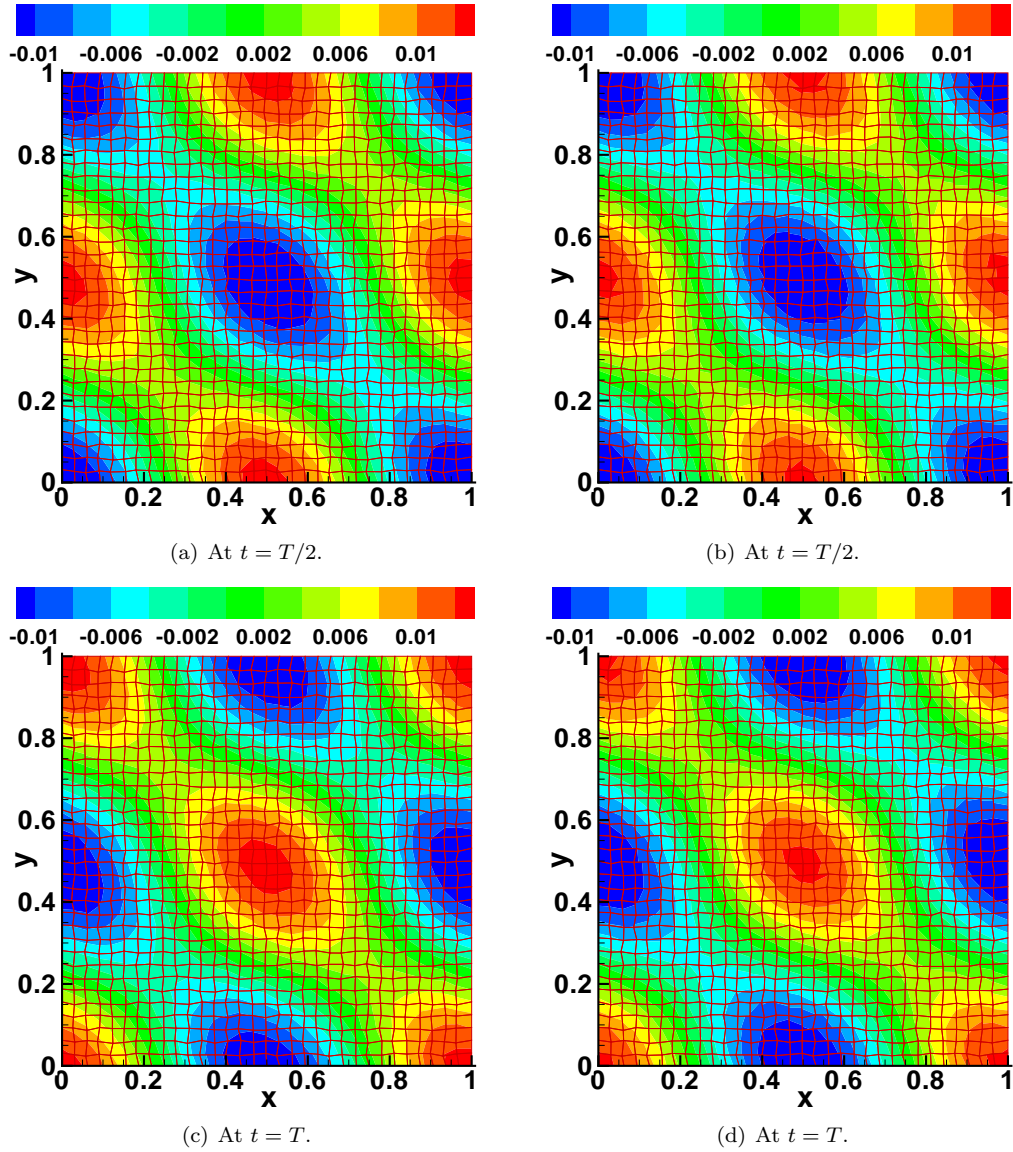
(b) At $t = T/2$.

(c) At $t = T$.

(d) At $t = T$.

Figure 5: Contour plots of the velocity potential on the mean free surface obtained with the space-time variational scheme (left) and the space-time DG scheme (right). These results are obtained on an irregular grid of size $32 \times 32 \times 8$ with time step $\Delta t = T/40$, where $T$ is the time period of the harmonic waves.

21

(a) At $t = T/2$.

(b) At $t = T/2$.
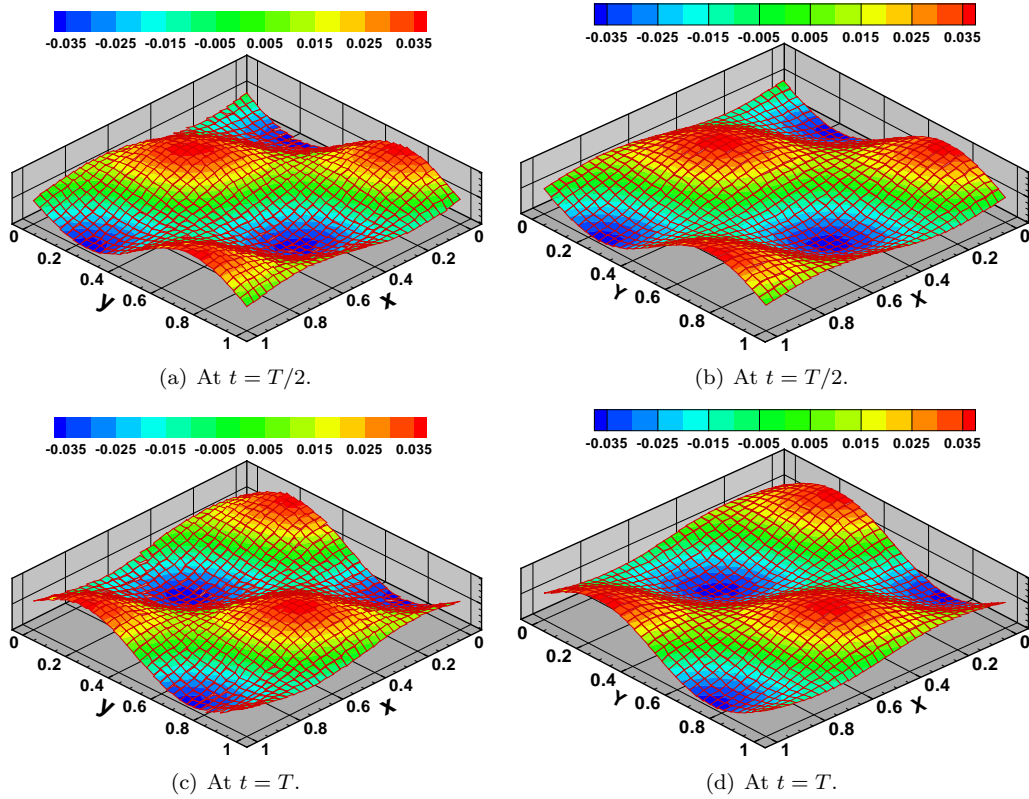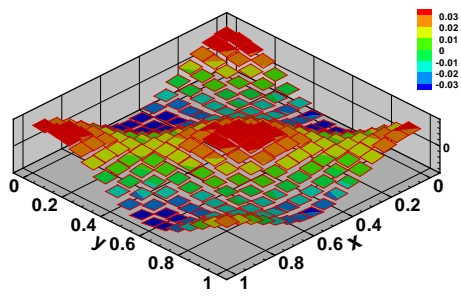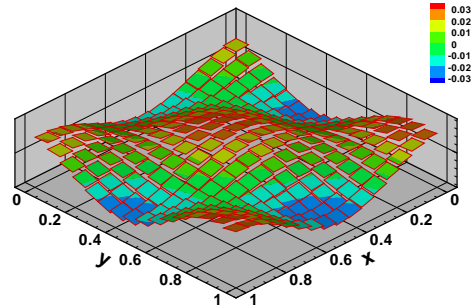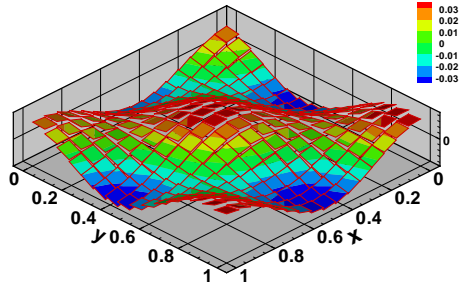
(c) At $t = T$.

(d) At $t = T$.

Figure 6: Contour plots of the free surface wave height obtained with the space-time variational scheme (left) and the space-time DG scheme (right). These results are obtained on an irregular grid of size $32 \times 32 \times 8$ with time step $\Delta t = T/40$, where $T$ is the time period of the harmonic waves.
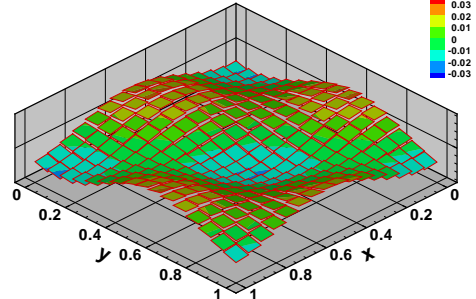
22

(a) At $t = T$.

(b) At $t = T$.

(c) At $t = 2T$.

(d) At $t = 2T$.

(e) At $t = 4T$.
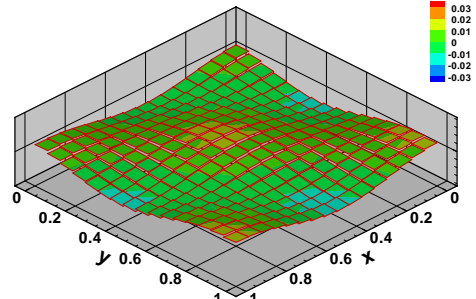
(f) At $t = 4T$.
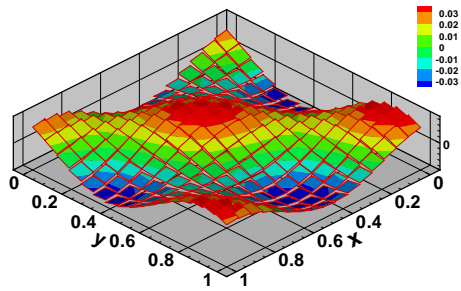
(g) At $t = 8T$
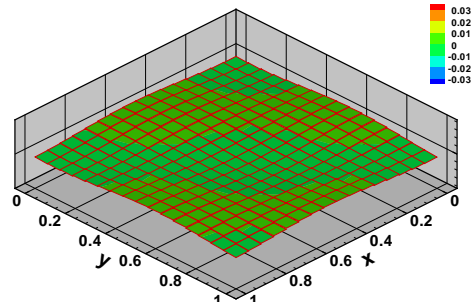
(h) At $t = 8T$

Figure 7: Contour plots of the free surface height obtained using space-time variational scheme (left) and space-time DG scheme (right). These results are obtained on an irregular grid of size $16 \times 16 \times 4$ with time step $\Delta t =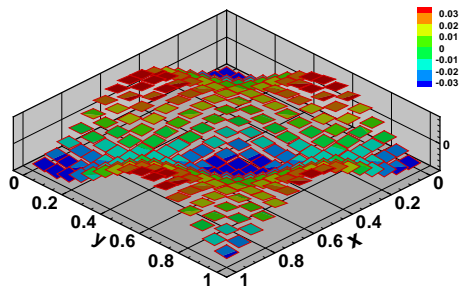 T/10$, where $T$ is the time period of the harmonic wave. Observe the decay of wave amplitude for space-time DG schemes.

23

slip flow boundary conditions at the remaining solid wall boundaries. We set the parameters $H = 1$, $l = 0$, $m = 1$ and $A = 2.32 \cdot 10^{-4}$ and simulate the waves for one time period $T = 2\pi/\omega = 2.4763$ with time step $\Delta t = T/10$, $T/20$, $T/40$ and $T/80$ for computational grids of size $8 \times 8 \times 2$, $16 \times 16 \times 4$, $32 \times 32 \times 8$ and $64 \times 64 \times 16$. The simulations were again performed with both the space-time DG scheme and space-time variational scheme. The numerical results obtained are compared with the exact solutions and the errors in the $L^2$–norm are computed to verify the order of accuracy of both schemes. The errors in the $L^2$–norm and the orders of accuracy are presented in Tables 3–6 for both the velocity potential and the free surface height. The free surface waves generated by a wave maker are shown in Figs. 8(a)-(j) and 9(a)-(j) simulated with the space-time DG scheme and space-time variational scheme, respectively. Again, we verified that both schemes obtain higher-order accuracy.

Table 3: $L^2$–errors of the velocity potential and the free surface height at $t = T$ on regular grids with the space-time DG scheme. Piston wavemaker case.

| Grid $N_x \times N_y \times N_z$ | Cell size h | Velocity potential $L^2$–error | order | Free surface height $L^2$–error | order |
|---|---|---|---|---|---|
| $8 \times 8 \times 2$ | 0.785155 | $3.9801 \cdot 10^{-04}$ | – | $5.0199 \cdot 10^{-03}$ | – |
| $16 \times 16 \times 4$ | 0.465848 | $7.4137 \cdot 10^{-05}$ | 3.22 | $1.5546 \cdot 10^{-03}$ | 1.69 |
| $32 \times 32 \times 8$ | 0.252864 | $2.0123 \cdot 10^{-05}$ | 2.13 | $3.9705 \cdot 10^{-04}$ | 1.97 |
| $64 \times 64 \times 16$ | 0.131652 | $5.3061 \cdot 10^{-06}$ | 2.04 | $9.8416 \cdot 10^{-05}$ | 2.01 |

Table 4: $L^2$–errors of the velocity potential and the free surface height at $t = T$ on irregular grids with the space-time DG scheme. Piston wavemaker case.

| Grid size $N_x \times N_y \times N_z$ | Cell size h | Velocity potential $L^2$–error | order | Free surface height $L^2$–error | order |
|---|---|---|---|---|---|
| $8 \times 8 \times 2$ | 0.795757 | $3.9649 \cdot 10^{-04}$ | – | $4.9753 \cdot 10^{-03}$ | – |
| $16 \times 16 \times 4$ | 0.470324 | $7.5895 \cdot 10^{-05}$ | 3.14 | $1.4990 \cdot 10^{-03}$ | 1.73 |
| $32 \times 32 \times 8$ | 0.255019 | $2.0966 \cdot 10^{-05}$ | 2.10 | $3.0505 \cdot 10^{-04}$ | 2.30 |
| $64 \times 64 \times 16$ | 0.132687 | $5.3061 \cdot 10^{-06}$ | 2.08 | $9.8416 \cdot 10^{-05}$ | 1.63 |

# 8    Concluding remarks

A novel space-time variational (dis)continuous Galerkin method has been presented for irrotational dynamics of linear free surface waves. It is based on a novel numerical discretization of a variational principle. To achieve such a variational formulation, we derived a discrete functional which is analogous to that of the continuum case for linear free surface waves. The variational discretization preserves the advantageous features of the space-time DG scheme such as the locality of the discretization. In addition, it ensured the resulting system to be symmetric leading to a speed-up in the computation, and conservation of energy and phase space.
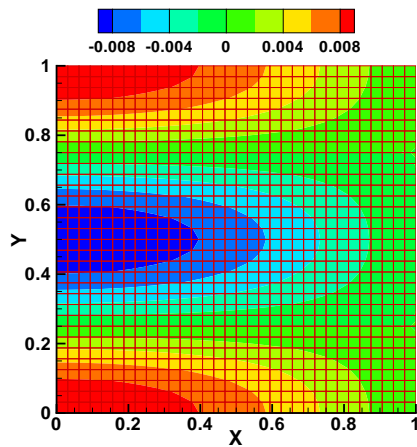
For comparison, we considered the space-time DG of van der Vegt and Xu [26], extended with novel numerical tests in three space dimensions. The numerical discretization resulting from this method consists of linear systems of algebraic equations with a compact stencil. It also allowed

Table 5: $L^2$–errors of the velocity potential and the free surface height at $t = T$ on regular grids with a $p^{\text{th}}$–order polynomial approximation (variational space-time DG scheme). Piston wavemaker case.

| Grid $N_x \times N_y \times N_z$ | Cell size h | Velocity potential $L^2$–error | order | Free surface height $L^2$–error | order |
|---|---|---|---|---|---|
| For $p = 1$ | | | | | |
| $8 \times 8 \times 2$ | 0.785155 | $3.9906 \cdot 10^{-04}$ | – | $8.2652 \cdot 10^{-03}$ | – |
| $16 \times 16 \times 4$ | 0.465848 | $1.0063 \cdot 10^{-04}$ | 2.64 | $3.4336 \cdot 10^{-03}$ | 1.27 |
| $32 \times 32 \times 8$ | 0.252864 | $2.1776 \cdot 10^{-05}$ | 2.51 | $9.7198 \cdot 10^{-04}$ | 1.82 |
| $64 \times 64 \times 16$ | 0.131652 | $5.4312 \cdot 10^{-06}$ | 2.13 | $2.4843 \cdot 10^{-04}$ | 1.97 |
| For $p = 2$ | | | | | |
| $8 \times 8 \times 2$ | 0.785155 | $5.9045 \cdot 10^{-05}$ | – | $1.4284 \cdot 10^{-03}$ | – |
| $16 \times 16 \times 4$ | 0.465848 | $9.8501 \cdot 10^{-06}$ | 3.43 | $3.8402 \cdot 10^{-05}$ | 5.22 |
| $32 \times 32 \times 8$ | 0.252864 | $1.0729 \cdot 10^{-06}$ | 3.63 | $3.4868 \cdot 10^{-06}$ | 3.46 |

Table 6: $L^2$–errors of the velocity potential and the free surface height at $t = T$ on irregular grids with a $p^{\text{th}}$–order polynomial approximation (variational space-time DG scheme). Piston wavemaker case.
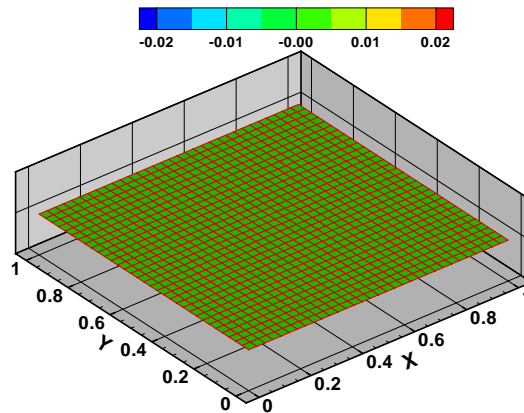
| Grid $N_x \times N_y \times N_z$ | Cell size h | Velocity potential $L^2$–error | order | Free surface height $L^2$–error | order |
|---|---|---|---|---|---|
| For $p = 1$ | | | | | |
| $8 \times 8 \times 2$ | 0.795757 | $4.0721 \cdot 10^{-04}$ | – | $4.9753 \cdot 10^{-03}$ | – |
| $16 \times 16 \times 4$ | 0.470324 | $1.0595 \cdot 10^{-04}$ | 2.56 | $1.4990 \cdot 10^{-03}$ | 1.64 |
| $32 \times 32 \times 8$ | 0.255019 | $2.3249 \cdot 10^{-05}$ | 2.48 | $3.0505 \cdot 10^{-04}$ | 1.95 |
| $64 \times 64 \times 16$ | 0.132687 | $5.4312 \cdot 10^{-06}$ | 2.20 | $9.8416 \cdot 10^{-05}$ | 2.22 |
| For $p = 2$ | | | | | |
| $8 \times 8 \times 2$ | 0.795757 | $6.1241 \cdot 10^{-05}$ | – | $1.1596 \cdot 10^{-03}$ | – |
| $16 \times 16 \times 4$ | 0.470324 | $1.0740 \cdot 10^{-05}$ | 3.31 | $1.5702 \cdot 10^{-04}$ | 3.80 |

(a) At $t = 0$.

(b) At $t = 0$.

(c) At $t = 2T/5$.

(d) At $t = 2T/5$.

(e) At $t = T/2$.

(f) At $t = T/2$.

26

(g) At $t = 4T/5$.



(h) At $t = 4T/5$.



(i) At $t = T$.



(j) At $t = T$.

Figure 8: Contour plots of the velocity potential $\phi_h$ at the mean free surface (left) and the free surface height $\eta_h$ (right) on a regular grid of size $32 \times 32 \times 8$ (Space-time DG scheme). Piston wavemaker case.



(a) At $t = 0$.



(b) At $t = 0$.
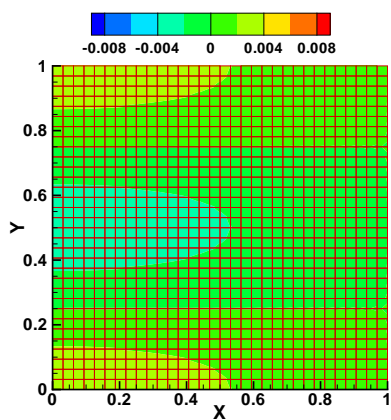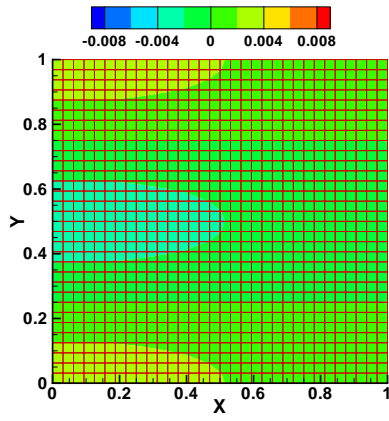
(c) At $t = 2T/5$.
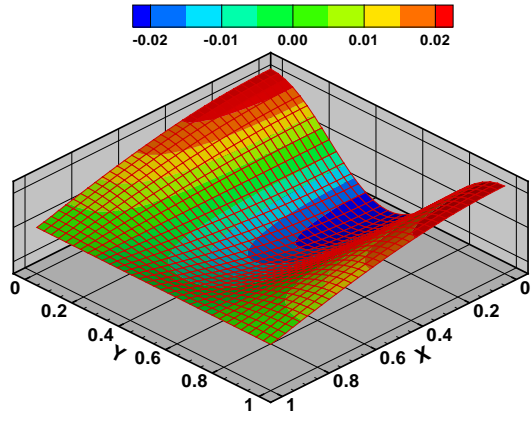


(d) At $t = 2T/5$.
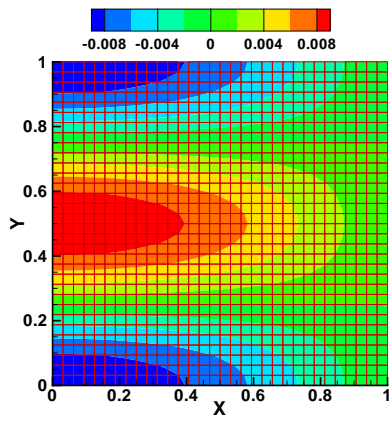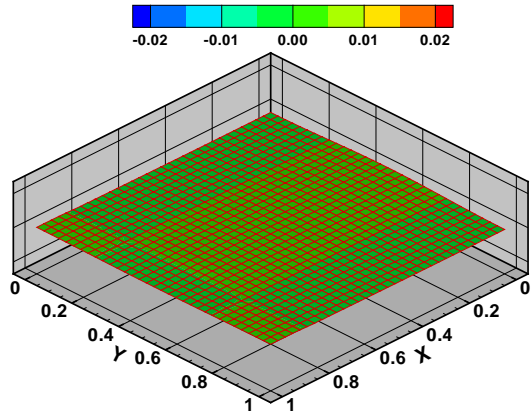


(e) At $t = T/2$.



(f) At $t = T/2$.



(g) At $t = 4T/5$.



(h) At $t = 4T/5$.

(i) At $t = T$.  (j) At $t = T$.
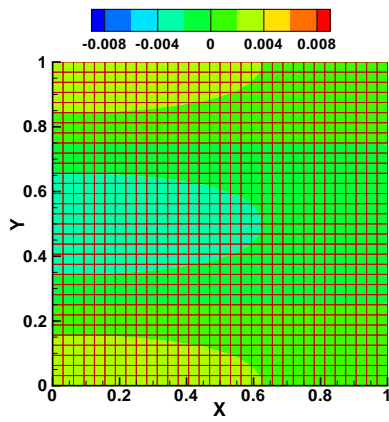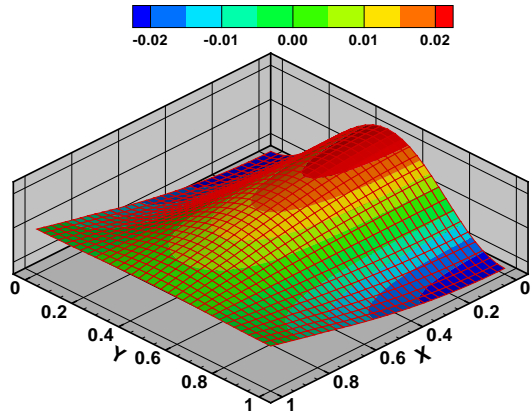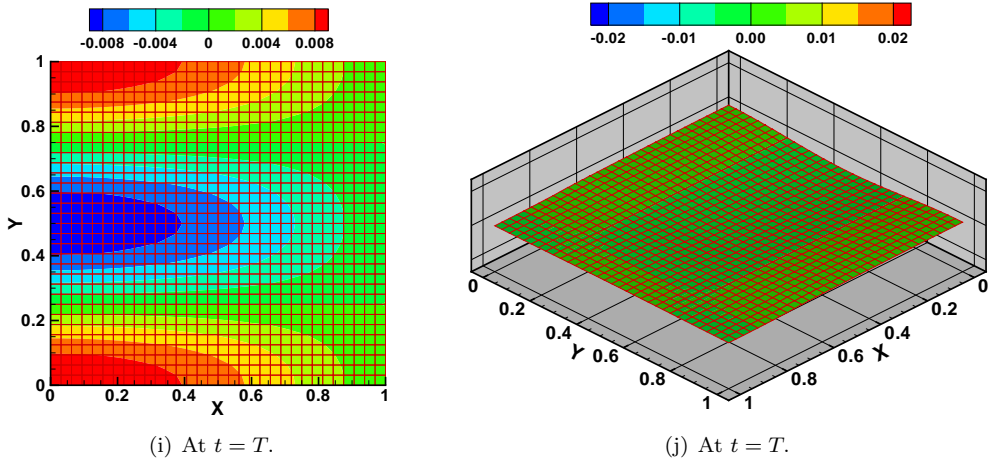
Figure 9: Contour plots of the velocity potential $\phi_{\mathsf{h}}$ at the mean free surface (left) and the free surface height $\eta_{\mathsf{h}}$ (right) on a regular grid of size $32 \times 32 \times 8$ (space-time variational scheme). Piston wavemaker case.
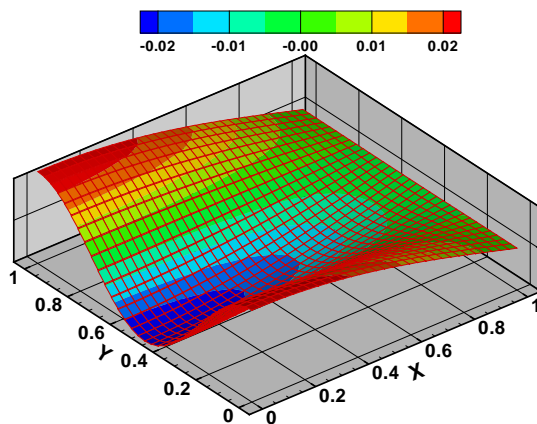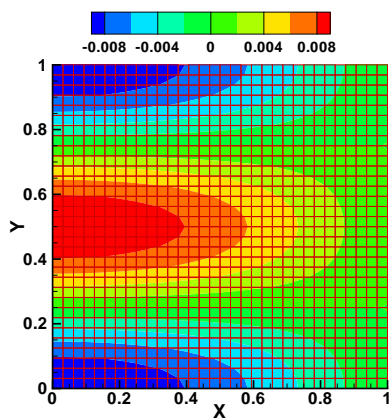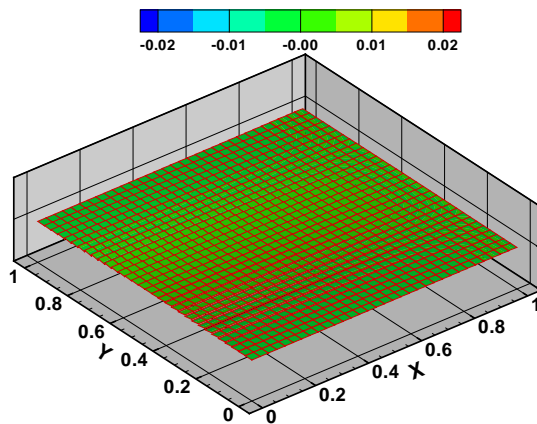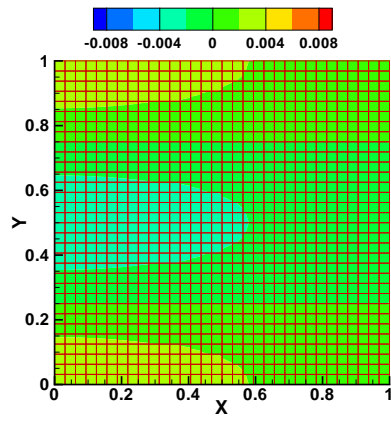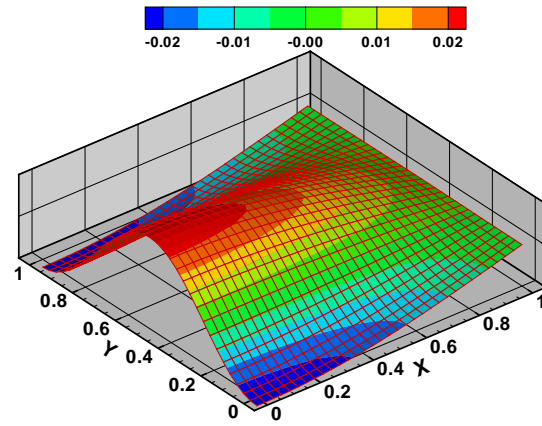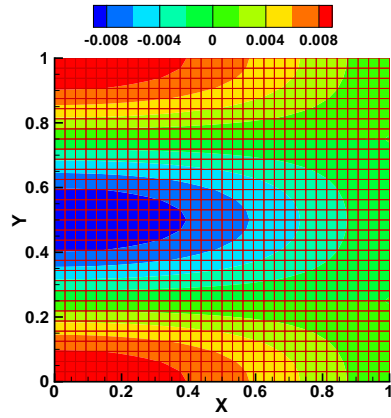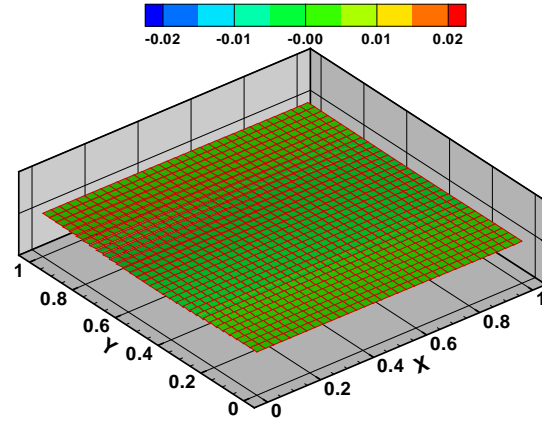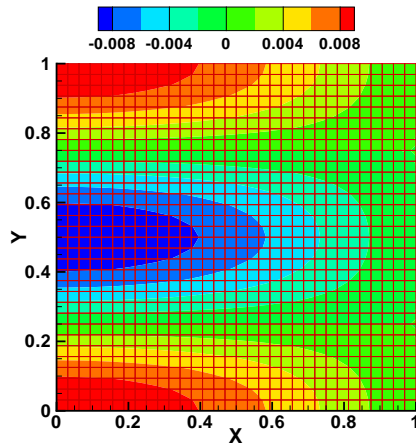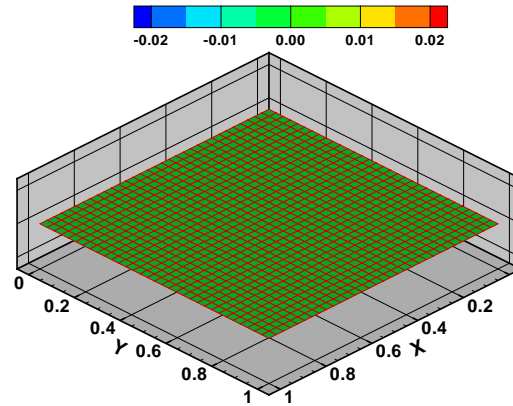
us to use efficient sparse matrix storage routines and iterative linear solvers in the PETSc package. The PETSc package gave a good performance relative to other methods, such as direct solvers and locally build and optimized conjugate gradient solvers. We found that preallocation of memory for the matrix storage rather than a dynamic memory allocation improves the performance of the package. An extra advantage of PETSc is that the parallelization is a built-in feature.

The numerical results of the space-time DG and variational schemes have been compared with exact solutions of linear harmonic free surface waves in a periodic domain and linear waves generated by a wave maker. Both schemes show $(p + 1)^{\text{th}}$–order accurate results for a $p^{\text{th}}$–order polynomial approximation of the wave field. Further, the space-time variational DG scheme does not show any decay in the amplitude of the waves whereas the space-time DG scheme shows significant amount of decay in the wave amplitude. However, the space-time variational DG finite element scheme shows a larger dispersion error. We recommend, therefore, to extend the space-time variational (dis)continuous Galerkin scheme to nonlinear free surface waves. And to further investigate the time discretization in the space-time variational method to improve the dispersion accuracy while preserving the zero amplitude decay.

# A  Appendix

## A.1  Space-time DG discretization

In this Appendix, we present the space-time finite element discretization of the space-time discontinuous Galerkin weak formulation (61) by substituting the polynomial expansions for the velocity potential $\phi_{\mathsf{h}}$, the free surface height $\eta_{\mathsf{h}}$ and the local lifting operator $\mathcal{R}_{\mathcal{S},\mathsf{k}}(\llbracket \phi \rrbracket)$ in (61), and choosing the test functions $v_{\mathsf{h}}$ and $w_{\mathsf{h}}$ as $\psi_{\mathsf{k},i}$ and $\varphi_{\mathsf{l},i}$, respectively.

First, we present the discretization of the bilinear form $B_{\mathsf{h}}(\phi_{\mathsf{h}}, v)$ in (61) is as follows:

$$B_{\mathsf{h}}(\phi_{\mathsf{h}}, \psi_i) := \sum_{\mathsf{k}=1}^{N_e} \sum_{j=1}^{n_p} \hat{\phi}_{\mathsf{k},j} \int_{\mathcal{K}_{\mathsf{k}}^n} \bar{\nabla}\psi_{\mathsf{k},j} \cdot \bar{\nabla}\psi_{\mathsf{k},i} \, \mathrm{d}\mathcal{K}$$

$$- \sum_{\mathcal{S} \in \Gamma_{int}} \sum_{j=1}^{n_p} \Big( \frac{1}{2} \hat{\phi}_{\mathsf{l},j} \int_{\mathcal{S}} \psi_{\mathsf{l},j} (\bar{\mathbf{n}}^{\mathsf{l}} \cdot \bar{\nabla}\psi_{\mathsf{l},i} + \bar{\mathbf{n}}^{\mathsf{l}} \cdot \bar{\nabla}\psi_{\mathsf{r},i}) \, \mathrm{d}\mathcal{S}$$

29

$$+ \frac{1}{2}\hat{\phi}_{\mathsf{r},j} \int_{\mathcal{S}} \psi_{\mathsf{r},j}(\bar{\mathbf{n}}^{\mathsf{r}} \cdot \bar{\nabla}\psi_{\mathsf{l},i} + \bar{\mathbf{n}}^{\mathsf{r}} \cdot \bar{\nabla}\psi_{\mathsf{r},i})\, \mathrm{d}\mathcal{S}\Big)$$

$$- \sum_{\mathcal{S}\in\Gamma_{int}} \sum_{j=1}^{n_p} \Big(\frac{1}{2}\hat{\phi}_{\mathsf{l},j} \int_{\mathcal{S}} ((\bar{\mathbf{n}}^l \cdot \bar{\nabla}\psi_{\mathsf{l},j})\psi_{\mathsf{l},i} + (\bar{\mathbf{n}}^r \cdot \bar{\nabla}\psi_{\mathsf{l},j})\psi_{\mathsf{r},i})\, \mathrm{d}\mathcal{S}$$

$$+ \frac{1}{2}\hat{\phi}_{\mathsf{r},j} \int_{\mathcal{S}} ((\bar{\mathbf{n}}^l \cdot \bar{\nabla}\psi_{\mathsf{r},j})\psi_{\mathsf{l},i} + (\bar{\mathbf{n}}^r \cdot \bar{\nabla}\psi_{\mathsf{r},j})\psi_{\mathsf{r},i})\, \mathrm{d}\mathcal{S}\Big)$$

$$- \sum_{\mathcal{S}\in\Gamma_{int}} \sum_{j=1}^{n_p} \sum_{k=1}^{3} n_{\mathcal{S}}\Big(\frac{1}{2}\hat{R}_{k,j}^{\mathcal{S},\mathsf{l}} \int_{\mathcal{S}} \big(n_k^{\mathsf{l}}\psi_{\mathsf{l},j}\psi_{\mathsf{l},i} + n_k^{\mathsf{r}}\psi_{\mathsf{l},j}\psi_{\mathsf{r},i}\big)\, \mathrm{d}\mathcal{S}$$

$$+ \frac{1}{2}\hat{R}_{k,j}^{\mathcal{S},\mathsf{r}} \int_{\mathcal{S}} \big(n_k^{\mathsf{l}}\psi_{\mathsf{r},j}\psi_{\mathsf{l},i} + n_k^{\mathsf{r}}\psi_{\mathsf{r},j}\psi_{\mathsf{r},i}\big)\, \mathrm{d}\mathcal{S}\Big). \tag{100}$$

Second, the discretization of the linear form and the other free surface terms of the first equation in (61) is

$$L_{\mathsf{h}}(\psi_i) = \sum_{\mathcal{S}\in\Gamma_L} \int_{\mathcal{S}} g_N \psi_i\, \mathrm{d}\mathcal{S}, \quad (\partial_t \eta_{\mathsf{h}}, \psi_i)_{\Gamma_S} = \sum_{\mathcal{S}\in\Gamma_S} \sum_{j=1}^{n_q} \hat{\eta}_{\mathsf{l},j}^n \int_{\mathcal{S}} (\partial_t \varphi_{\mathsf{l},j})\psi_{\mathsf{l},i}\, \mathrm{d}\mathcal{S} \quad \text{and}$$

$$\big(\eta^- - \eta^+, \psi_i\big)_{\Gamma_S(t_{n-1}^-)} = \sum_{\mathcal{S}\in\Gamma_S} \sum_{j=1}^{n_q} \Big(\hat{\eta}_{\mathsf{l},j}^n \int_{\partial\mathcal{S}(t_{n-1}^-)} \varphi_{\mathsf{l},j}\psi_{\mathsf{l},i}\, \mathrm{d}(\partial\mathcal{S}) - \hat{\eta}_{\mathsf{r},j}^{n-1} \int_{\partial\mathcal{S}(t_{n-1}^-)} \varphi_{\mathsf{l},j}\psi_{\mathsf{l},i}\, \mathrm{d}(\partial\mathcal{S})\Big). \tag{101}$$

Finally, the discretization of the second equation in (61) is given as

$$\sum_{\mathcal{S}\in\Gamma_S} \sum_{j=1}^{n_p} \Big(\phi_{\mathsf{l},j}^n \int_{\mathcal{S}} (\partial_t\psi_{\mathsf{l},j})\varphi_{\mathsf{l},i}\, \mathrm{d}\mathcal{S} + \hat{\phi}_{\mathsf{l},j}^n \int_{\partial\mathcal{S}(t_{n-1}^-)} \psi_{\mathsf{l},j}\varphi_{\mathsf{l},i}\, \mathrm{d}(\partial\mathcal{S})$$

$$- \hat{\phi}_{\mathsf{r},j}^{n-1} \int_{\partial\mathcal{S}(t_{n-1}^-)} \psi_{\mathsf{r},j}\varphi_{\mathsf{l},i}\, \mathrm{d}(\partial\mathcal{S}) + \hat{\eta}_{\mathsf{l},j}^n \int_{\mathcal{S}} \varphi_{\mathsf{l},j}\varphi_{\mathsf{l},i}\, \mathrm{d}\mathcal{S}\Big) = 0. \tag{102}$$

To obtain and describe the linear system of algebraic equations resulting from (100) to (102), we introduce and use the following matrix and vector notations:

$$A_{ij}^{\mathcal{K},\mathsf{k}} := \int_{\mathcal{K}_{\mathsf{k}}} \psi_{\mathsf{k},i}\psi_{\mathsf{k},j}\mathrm{d}\mathcal{K}, \qquad\qquad B_{ij}^{\mathcal{K},\mathsf{kk}} := \int_{\mathcal{K}_{\mathsf{k}}} \bar{\nabla}\psi_{\mathsf{k},i} \cdot \bar{\nabla}\psi_{\mathsf{k},j}\mathrm{d}\mathcal{K},$$

$$C_{ij}^{\mathcal{S},\mathsf{lr}} := \int_{\mathcal{S}} (\bar{\mathbf{n}}^\mathsf{l} \cdot \bar{\nabla}\psi_{\mathsf{l},i})\, \psi_{\mathsf{r},j}\mathrm{d}\mathcal{S}, \qquad\qquad D_{k,ij}^{\mathcal{S},\mathsf{lr}} := \int_{\mathcal{S}} n_k^{\mathsf{l}}\psi_{\mathsf{l},i}\psi_{\mathsf{r},j}\mathrm{d}\mathcal{S},$$

$$F_i^{\mathcal{S},\phi} := \hat{\phi}_{\mathsf{r},j}^{n-1} \int_{\partial\mathcal{S}(t_{n-1}^-)} \psi_{\mathsf{r},j}\varphi_{\mathsf{l},i}\, \mathrm{d}(\partial\mathcal{S}), \qquad\qquad H_{ij}^{\mathcal{S}} := \int_{\mathcal{S}} \varphi_{\mathsf{l},j}\varphi_{\mathsf{l},i}\, \mathrm{d}\mathcal{S},$$

$$F_i^{\mathcal{S},\eta} := \hat{\eta}_{\mathsf{r},j}^{n-1} \int_{\partial\mathcal{S}(t_{n-1}^-)} \varphi_{\mathsf{r},j}\psi_{\mathsf{l},i}\, \mathrm{d}(\partial\mathcal{S}), \qquad\qquad E_i^{\mathcal{S},\mathsf{l}} := \int_{\mathcal{S}_{\mathsf{m}}} g_N \psi_{\mathsf{l},i}\mathrm{d}\mathcal{S},$$

$$G_{ij}^{\mathcal{S}} := \int_{\mathcal{S}} (\partial_t\psi_{\mathsf{l},j})\varphi_{\mathsf{l},i}\, \mathrm{d}\mathcal{S} + \int_{\partial\mathcal{S}(t_{n-1}^-)} \psi_{\mathsf{l},j}\varphi_{\mathsf{l},i}\, \mathrm{d}(\partial\mathcal{S}),$$

$$\bar{G}_{ij}^{\mathcal{S}} := \int_{\mathcal{S}} (\partial_t\varphi_{\mathsf{l},j})\psi_{\mathsf{l},i}\, \mathrm{d}\mathcal{S} + \int_{\partial\mathcal{S}(t_{n-1}^-)} \varphi_{\mathsf{l},j}\psi_{\mathsf{l},i}\, \mathrm{d}(\partial\mathcal{S}),$$

$$M^{\mathsf{ll}} := \sum_{k=1}^{3} \Big(D_k^{\mathcal{S},\mathsf{ll}}(A^{\mathcal{K},\mathsf{l}})^{-1}(D_k^{\mathcal{S},\mathsf{ll}})^T + D_k^{\mathcal{S},\mathsf{lr}}(A^{\mathcal{K},\mathsf{r}})^{-1}(D_k^{\mathcal{S},\mathsf{rl}})^T\Big),$$

$$M^{\mathsf{lr}} := \sum_{k=1}^{3} \Big(D_k^{\mathcal{S},\mathsf{ll}}(A^{\mathcal{K},\mathsf{l}})^{-1}(D_k^{\mathcal{S},\mathsf{rl}})^T + D_k^{\mathcal{S},\mathsf{lr}}(A^{\mathcal{K},\mathsf{r}})^{-1}(D_k^{\mathcal{S},\mathsf{rr}})^T\Big),$$

30

$$M^{\mathsf{rl}} := \sum_{k=1}^{3} \left( D_k^{\mathcal{S},\mathsf{rl}} (A^{\mathcal{K},\mathsf{l}})^{-1} (D_k^{\mathcal{S},\mathsf{ll}})^T + D_k^{\mathcal{S},\mathsf{rr}} (A^{\mathcal{K},\mathsf{r}})^{-1} (D_k^{\mathcal{S},\mathsf{lr}})^T \right),$$

$$M^{\mathsf{rr}} := \sum_{k=1}^{3} \left( D_k^{\mathcal{S},\mathsf{rl}} (A^{\mathcal{K},\mathsf{l}})^{-1} (D_k^{\mathcal{S},\mathsf{rl}})^T + D_k^{\mathcal{S},\mathsf{rr}} (A^{\mathcal{K},\mathsf{r}})^{-1} (D_k^{\mathcal{S},\mathsf{rr}})^T \right). \tag{103}$$

## A.2  Space-time variational discretization

In this Appendix, we present the space-time variational discretization of the variational formulation (81) and (82) by substituting the polynomial expansion of the velocity potential $\phi_{\mathsf{h}}$, the free surface height $\eta_{\mathsf{h}}$ and the local lifting operator $\mathcal{R}_{\mathcal{S},\mathsf{k}}(\llbracket \phi \rrbracket)$ (84) into the variational formulation (81) and (82), and choosing the arbitrariness of the variations $\delta \bar{\phi}_{\mathsf{h}}^n$ and $\delta \bar{\eta}_{\mathsf{h}}$ as $\psi^n \psi^{n-1} \bar{\psi}_{\mathsf{k},i}$ and $\psi^n \psi^{n-1} \bar{\varphi}_{\mathsf{l},i}$, respectively. Now, the space-time variational discretization of the variational formulation (81) using (87) is as follows:

$$\sum_{\mathcal{K}} \sum_{j=1}^{n_p} \hat{\phi}_{\mathsf{k},j}^n \int_{\mathcal{K}_{\mathsf{k}}^n} (\psi_{\mathsf{k}}^n)^2 \psi_{\mathsf{k}}^{n-1} (\bar{\nabla} \bar{\psi}_{\mathsf{k},j} \cdot \bar{\nabla} \bar{\psi}_{\mathsf{k},i}) \, \mathrm{d}\mathcal{K} +$$

$$\sum_{\mathcal{K}} \sum_{j=1}^{n_p} \hat{\phi}_{\mathsf{k},j}^{n-1} \int_{\mathcal{K}_{\mathsf{k}}^n} \psi_{\mathsf{k}}^n (\psi_{\mathsf{k}}^{n-1})^2 (\bar{\nabla} \bar{\psi}_{\mathsf{k},j} \cdot \bar{\nabla} \bar{\psi}_{\mathsf{k},i}) \, \mathrm{d}\mathcal{K}$$

$$- \sum_{\mathcal{S} \in \Gamma_{int}} \sum_{j=1}^{n_p} \left( \frac{1}{2} \hat{\phi}_{\mathsf{l},j}^n \int_{\mathcal{S}} \psi_{\mathsf{l}}^n \bar{\psi}_{\mathsf{l},j} \left( \psi_{\mathsf{l}}^n \psi_{\mathsf{l}}^{n-1} (\bar{\mathbf{n}}^{\mathsf{l}} \cdot \bar{\nabla} \bar{\psi}_{\mathsf{l},i}) + \psi_{\mathsf{r}}^n \psi_{\mathsf{r}}^{n-1} (\bar{\mathbf{n}}^{\mathsf{l}} \cdot \bar{\nabla} \bar{\psi}_{\mathsf{r},i}) \right) \, \mathrm{d}\mathcal{S} \right.$$

$$\left. + \frac{1}{2} \hat{\phi}_{\mathsf{r},j}^n \int_{\mathcal{S}} \psi_{\mathsf{r}}^n \bar{\psi}_{\mathsf{r},j} \left( \psi_{\mathsf{l}}^n \psi_{\mathsf{l}}^{n-1} (\bar{\mathbf{n}}^{\mathsf{r}} \cdot \bar{\nabla} \bar{\psi}_{\mathsf{l},i}) + \psi_{\mathsf{r}}^n \psi_{\mathsf{r}}^{n-1} (\bar{\mathbf{n}}^{\mathsf{r}} \cdot \bar{\nabla} \bar{\psi}_{\mathsf{r},i}) \right) \, \mathrm{d}\mathcal{S} \right)$$

$$- \sum_{\mathcal{S} \in \Gamma_{int}} \sum_{j=1}^{n_p} \left( \frac{1}{2} \hat{\phi}_{\mathsf{l},j}^{n-1} \int_{\mathcal{S}} \psi_{\mathsf{l}}^{n-1} \bar{\psi}_{\mathsf{l},j} \left( \psi_{\mathsf{l}}^n \psi_{\mathsf{l}}^{n-1} (\bar{\mathbf{n}}^{\mathsf{l}} \cdot \bar{\nabla} \bar{\psi}_{\mathsf{l},i}) + \psi_{\mathsf{r}}^n \psi_{\mathsf{r}}^{n-1} (\bar{\mathbf{n}}^{\mathsf{l}} \cdot \bar{\nabla} \bar{\psi}_{\mathsf{r},i}) \right) \, \mathrm{d}\mathcal{S} \right.$$

$$\left. + \frac{1}{2} \hat{\phi}_{\mathsf{r},j}^{n-1} \int_{\mathcal{S}} \psi_{\mathsf{r}}^{n-1} \bar{\psi}_{\mathsf{r},j} \left( \psi_{\mathsf{l}}^n \psi_{\mathsf{l}}^{n-1} (\bar{\mathbf{n}}^{\mathsf{r}} \cdot \bar{\nabla} \bar{\psi}_{\mathsf{l},i}) + \psi_{\mathsf{r}}^n \psi_{\mathsf{r}}^{n-1} (\bar{\mathbf{n}}^{\mathsf{r}} \cdot \bar{\nabla} \bar{\psi}_{\mathsf{r},i}) \right) \, \mathrm{d}\mathcal{S} \right)$$

$$- \sum_{\mathcal{S} \in \Gamma_{int}} \sum_{j=1}^{n_p} \left( \frac{1}{2} \hat{\phi}_{\mathsf{l},j}^n \int_{\mathcal{S}} \psi_{\mathsf{l}}^n \left( \psi_{\mathsf{l}}^n \psi_{\mathsf{l}}^{n-1} (\bar{\mathbf{n}}^{\mathsf{l}} \cdot \bar{\nabla} \bar{\psi}_{\mathsf{l},j}) \bar{\psi}_{\mathsf{l},i} + \psi_{\mathsf{r}}^n \psi_{\mathsf{r}}^{n-1} (\bar{\mathbf{n}}^{\mathsf{r}} \cdot \bar{\nabla} \bar{\psi}_{\mathsf{l},j}) \bar{\psi}_{\mathsf{r},i} \right) \, \mathrm{d}\mathcal{S} \right.$$

$$\left. + \frac{1}{2} \hat{\phi}_{\mathsf{r},j}^n \int_{\mathcal{S}} \psi_{\mathsf{r}}^n \left( \psi_{\mathsf{l}}^n \psi_{\mathsf{l}}^{n-1} (\bar{\mathbf{n}}^{\mathsf{l}} \cdot \bar{\nabla} \bar{\psi}_{\mathsf{r},j}) \bar{\psi}_{\mathsf{l},i} + \psi_{\mathsf{r}}^n \psi_{\mathsf{r}}^{n-1} (\bar{\mathbf{n}}^{\mathsf{r}} \cdot \bar{\nabla} \bar{\psi}_{\mathsf{r},j}) \bar{\psi}_{\mathsf{r},i} \right) \, \mathrm{d}\mathcal{S} \right)$$

$$- \sum_{\mathcal{S} \in \Gamma_{int}} \sum_{j=1}^{n_p} \left( \frac{1}{2} \hat{\phi}_{\mathsf{l},j}^{n-1} \int_{\mathcal{S}} \psi_{\mathsf{l}}^{n-1} \left( \psi_{\mathsf{l}}^n \psi_{\mathsf{l}}^{n-1} (\bar{\mathbf{n}}^{\mathsf{l}} \cdot \bar{\nabla} \bar{\psi}_{\mathsf{l},j}) \bar{\psi}_{\mathsf{l},i} + \psi_{\mathsf{r}}^n \psi_{\mathsf{r}}^{n-1} (\bar{\mathbf{n}}^{\mathsf{r}} \cdot \bar{\nabla} \bar{\psi}_{\mathsf{l},j}) \bar{\psi}_{\mathsf{r},i} \right) \, \mathrm{d}\mathcal{S} \right.$$

$$\left. + \frac{1}{2} \hat{\phi}_{\mathsf{r},j}^{n-1} \int_{\mathcal{S}} \psi_{\mathsf{r}}^{n-1} \left( \psi_{\mathsf{l}}^n \psi_{\mathsf{l}}^{n-1} (\bar{\mathbf{n}}^{\mathsf{l}} \cdot \bar{\nabla} \bar{\psi}_{\mathsf{r},j}) \bar{\psi}_{\mathsf{l},i} + \psi_{\mathsf{r}}^n \psi_{\mathsf{r}}^{n-1} (\bar{\mathbf{n}}^{\mathsf{r}} \cdot \bar{\nabla} \bar{\psi}_{\mathsf{r},j}) \bar{\psi}_{\mathsf{r},i} \right) \, \mathrm{d}\mathcal{S} \right)$$

$$- \sum_{\mathcal{S} \in \Gamma_{int}} \sum_{j=1}^{n_p} \sum_{k=1}^{3} n_{\mathcal{S}} \left( \frac{1}{2} \hat{R}_{k,j}^{\mathcal{S},\mathsf{ln}} \int_{\mathcal{S}} \psi_{\mathsf{l}}^n \left( \psi_{\mathsf{l}}^n \psi_{\mathsf{l}}^{n-1} n_k^{\mathsf{l}} \bar{\psi}_{\mathsf{l},j} \bar{\psi}_{\mathsf{l},i} + \psi_{\mathsf{r}}^n \psi_{\mathsf{r}}^{n-1} n_k^{\mathsf{r}} \bar{\psi}_{\mathsf{l},j} \bar{\psi}_{\mathsf{r},i} \right) \, \mathrm{d}\mathcal{S} \right.$$

$$\left. + \frac{1}{2} \hat{R}_{k,j}^{\mathcal{S},\mathsf{rn}} \int_{\mathcal{S}} \psi_{\mathsf{r}}^n \left( \psi_{\mathsf{l}}^n \psi_{\mathsf{l}}^{n-1} n_k^{\mathsf{l}} \bar{\psi}_{\mathsf{r},j} \bar{\psi}_{\mathsf{l},i} + \psi_{\mathsf{r}}^n \psi_{\mathsf{r}}^{n-1} n_k^{\mathsf{r}} \bar{\psi}_{\mathsf{r},j} \bar{\psi}_{\mathsf{r},i} \right) \, \mathrm{d}\mathcal{S} \right)$$

$$- \sum_{\mathcal{S} \in \Gamma_{int}} \sum_{j=1}^{n_p} \sum_{k=1}^{3} n_{\mathcal{S}} \left( \frac{1}{2} \hat{R}_{k,j}^{\mathcal{S},\mathsf{ln}-1} \int_{\mathcal{S}} \psi_{\mathsf{l}}^{n-1} \left( \psi_{\mathsf{l}}^n \psi_{\mathsf{l}}^{n-1} n_k^{\mathsf{l}} \bar{\psi}_{\mathsf{l},j} \bar{\psi}_{\mathsf{l},i} + \psi_{\mathsf{r}}^n \psi_{\mathsf{r}}^{n-1} n_k^{\mathsf{r}} \bar{\psi}_{\mathsf{l},j} \bar{\psi}_{\mathsf{r},i} \right) \, \mathrm{d}\mathcal{S} \right.$$

$$+ \frac{1}{2} \hat{R}_{k,j}^{\mathcal{S},\mathsf{r}n-1} \int_{\mathcal{S}} \psi_{\mathsf{r}}^{n-1} \Big( \psi_{\mathsf{l}}^{n} \psi_{\mathsf{l}}^{n-1} n_{k}^{\mathsf{l}} \bar{\psi}_{\mathsf{r},j} \bar{\psi}_{\mathsf{l},i} + \psi_{\mathsf{r}}^{n} \psi_{\mathsf{r}}^{n-1} n_{k}^{\mathsf{r}} \bar{\psi}_{\mathsf{r},j} \bar{\psi}_{\mathsf{r},i} \Big) \, \mathrm{d}\mathcal{S} \Big)$$

$$- \sum_{\mathcal{S}\in\Gamma_{L}} \sum_{j=1}^{n_{p}} \int_{\mathcal{S}} g_{N} \psi_{\mathsf{l}}^{n} \psi_{\mathsf{l}}^{n-1} \bar{\psi}_{\mathsf{l},i} \, \mathrm{d}\mathcal{S} - \sum_{\mathcal{S}\in\Gamma_{S}} \sum_{j=1}^{n_{p}} \hat{\eta}_{\mathsf{l},j}^{n} \int_{\mathcal{S}} \psi_{\mathsf{l}}^{n} \psi_{\mathsf{l}}^{n-1} (\partial_{t} \psi_{\mathsf{l},j}^{n}) \bar{\psi}_{\mathsf{l},i} \bar{\varphi}_{\mathsf{l},j} \, \mathrm{d}\mathcal{S}$$

$$- \sum_{\mathcal{S}\in\Gamma_{S}} \sum_{j=1}^{n_{p}} \hat{\eta}_{\mathsf{l},j}^{n-1} \int_{\mathcal{S}} \psi_{\mathsf{l}}^{n} \psi_{\mathsf{l}}^{n-1} (\partial_{t} \psi_{\mathsf{l}}^{n-1}) \bar{\psi}_{\mathsf{l},i} \bar{\varphi}_{\mathsf{l},j} \, \mathrm{d}\mathcal{S} = 0. \tag{104}$$

Next, the discretization of (82) is

$$\sum_{\mathcal{S}\in\Gamma_{S}} \sum_{j=1}^{n_{p}} \hat{\phi}_{\mathsf{l},j}^{n} \int_{\mathcal{S}} \psi_{\mathsf{l}}^{n} \big( \partial_{t} (\psi_{\mathsf{l}}^{n} \psi_{\mathsf{l}}^{n-1}) \big) \bar{\varphi}_{\mathsf{l},i} \bar{\psi}_{\mathsf{l},j} \, \mathrm{d}\mathcal{S} + \sum_{\mathcal{S}\in\Gamma_{S}} \sum_{j=1}^{n_{p}} \hat{\phi}_{\mathsf{l},j}^{n-1} \int_{\mathcal{S}} \psi_{\mathsf{l}}^{n-1} \big( \partial_{t} (\psi_{\mathsf{l}}^{n} \psi_{\mathsf{l}}^{n-1}) \big) \bar{\varphi}_{\mathsf{l},i} \bar{\psi}_{\mathsf{l},j} \, \mathrm{d}\mathcal{S} -$$

$$\sum_{\mathcal{S}\in\Gamma_{S}} \sum_{j=1}^{n_{p}} g \hat{\eta}_{\mathsf{l},j}^{n} \int_{\mathcal{S}} (\psi_{\mathsf{l}}^{n})^{2} \psi_{\mathsf{l}}^{n-1} \bar{\varphi}_{\mathsf{l},i} \bar{\psi}_{\mathsf{l},j} \, \mathrm{d}\mathcal{S} \sum_{\mathcal{S}\in\Gamma_{S}} \sum_{j=1}^{n_{p}} g \hat{\eta}_{\mathsf{l},j}^{n-1} \int_{\mathcal{S}} \psi_{\mathsf{l}}^{n} (\psi_{\mathsf{l}}^{n-1})^{2} \bar{\varphi}_{\mathsf{l},i} \bar{\psi}_{\mathsf{l},j} \, \mathrm{d}\mathcal{S} = 0. \tag{105}$$

To obtain and describe the linear system of algebraic equations from (104) and (105), we introduce and use the following matrix and vector notations:

$$A_{ij}^{\mathcal{K},\mathsf{k}} := \int_{\mathcal{K}_{\mathsf{k}}^{n}} \bar{\psi}_{\mathsf{k},i} \bar{\psi}_{\mathsf{k},j} \, \mathrm{d}\mathcal{K}, \qquad\qquad B_{ij}^{\mathcal{K},\mathsf{kk}} := \int_{\mathcal{K}_{\mathsf{k}}^{n}} (\psi_{\mathsf{k}}^{n})^{2} \psi_{\mathsf{k}}^{n-1} \bar{\nabla} \bar{\psi}_{\mathsf{k},i} \cdot \bar{\nabla} \bar{\psi}_{\mathsf{k},j} \, \mathrm{d}\mathcal{K},$$

$$\bar{B}_{ij}^{\mathcal{K},\mathsf{kk}} := \int_{\mathcal{K}_{\mathsf{k}}^{n}} (\psi_{\mathsf{k}}^{n-1})^{2} \psi_{\mathsf{k}}^{n} \bar{\nabla} \bar{\psi}_{\mathsf{k},i} \cdot \bar{\nabla} \bar{\psi}_{\mathsf{k},j} \, \mathrm{d}\mathcal{K}, \qquad\qquad C_{ij}^{\mathcal{S},\mathsf{lr}} := \int_{\mathcal{S}} \psi_{\mathsf{l}}^{n} \psi_{\mathsf{l}}^{n-1} \psi_{\mathsf{r}}^{n} (\bar{\mathbf{n}}^{\mathsf{l}} \cdot \bar{\nabla} \psi_{\mathsf{l},i}) \, \psi_{\mathsf{r},j} \mathrm{d}\mathcal{S},$$

$$\bar{C}_{ij}^{\mathcal{S},\mathsf{lr}} := \int_{\mathcal{S}} \psi_{\mathsf{l}}^{n} \psi_{\mathsf{l}}^{n-1} \psi_{\mathsf{r}}^{n-1} (\bar{\mathbf{n}}^{\mathsf{l}} \cdot \bar{\nabla} \psi_{\mathsf{l},i}) \, \psi_{\mathsf{r},j} \mathrm{d}\mathcal{S}, \qquad\qquad \hat{D}_{k,ij}^{\mathcal{S},\mathsf{lr}} := \int_{\mathcal{S}} n_{k}^{\mathsf{l}} \bar{\psi}_{\mathsf{l},i} \bar{\psi}_{\mathsf{r},j} \mathrm{d}\mathcal{S},$$

$$D_{k,ij}^{\mathcal{S},\mathsf{lr}} := \int_{\mathcal{S}} n_{k}^{\mathsf{l}} \psi_{\mathsf{l}}^{n} \psi_{\mathsf{l}}^{n-1} \psi_{\mathsf{r}}^{n} \bar{\psi}_{\mathsf{l},i} \bar{\psi}_{\mathsf{r},j} \mathrm{d}\mathcal{S}, \qquad\qquad \bar{D}_{k,ij}^{\mathcal{S},\mathsf{lr}} := \int_{\mathcal{S}} n_{k}^{\mathsf{l}} \psi_{\mathsf{l}}^{n} \psi_{\mathsf{l}}^{n-1} \psi_{\mathsf{r}}^{n-1} \bar{\psi}_{\mathsf{r},j} \bar{\psi}_{\mathsf{l},i} \mathrm{d}\mathcal{S},$$

$$G_{ij}^{\mathcal{S}} := \int_{\mathcal{S}} \psi_{\mathsf{l}}^{n} \psi_{\mathsf{l}}^{n-1} (\partial_{t} \psi_{\mathsf{l}}^{n}) \bar{\psi}_{\mathsf{l},i} \bar{\varphi}_{\mathsf{l},j} \, \mathrm{d}\mathcal{S}, \qquad\qquad \bar{G}_{ij}^{\mathcal{S}} := \int_{\mathcal{S}} \psi_{\mathsf{l}}^{n} \psi_{\mathsf{l}}^{n-1} (\partial_{t} \psi_{\mathsf{l}}^{n-1}) \bar{\psi}_{\mathsf{l},i} \bar{\varphi}_{\mathsf{l},j} \, \mathrm{d}\mathcal{S},$$

$$L_{ij}^{\mathcal{S}} := \int_{\mathcal{S}} \psi_{\mathsf{l}}^{n} \big( \partial_{t} (\psi_{\mathsf{l}}^{n} \psi_{\mathsf{l}}^{n-1}) \big) \bar{\varphi}_{\mathsf{l},i} \bar{\psi}_{\mathsf{l},j} \, \mathrm{d}\mathcal{S}, \qquad\qquad \bar{L}_{ij}^{\mathcal{S}} := \int_{\mathcal{S}} \psi_{\mathsf{l}}^{n-1} \big( \partial_{t} (\psi_{\mathsf{l}}^{n} \psi_{\mathsf{l}}^{n-1}) \big) \bar{\varphi}_{\mathsf{l},i} \bar{\psi}_{\mathsf{l},j} \, \mathrm{d}\mathcal{S},$$

$$H_{ij}^{\mathcal{S}} := \int_{\mathcal{S}} (\psi_{\mathsf{l}}^{n})^{2} \psi_{\mathsf{l}}^{n-1} \bar{\varphi}_{\mathsf{l},i} \bar{\varphi}_{\mathsf{l},j} \, \mathrm{d}\mathcal{S}, \qquad\qquad \bar{H}_{ij}^{\mathcal{S}} := \int_{\mathcal{S}} (\psi_{\mathsf{l}}^{n-1})^{2} \psi_{\mathsf{l}}^{n} \bar{\varphi}_{\mathsf{l},i} \bar{\varphi}_{\mathsf{l},j} \, \mathrm{d}\mathcal{S},$$

$$E_{i}^{\mathcal{S},\mathsf{l}} := \int_{\mathcal{S}_{\mathsf{m}}} g_{N} \psi_{\mathsf{l}}^{n} \psi_{\mathsf{l}}^{n-1} \psi_{\mathsf{l},i} \mathrm{d}\mathcal{S},$$

$$M^{\mathsf{ll}} := \sum_{k=1}^{3} \Big( D_{k}^{\mathcal{S},\mathsf{ll}} (A^{\mathcal{K},\mathsf{l}})^{-1} (\hat{D}_{k}^{\mathcal{S},\mathsf{ll}})^{T} + D_{k}^{\mathcal{S},\mathsf{lr}} (A^{\mathcal{K},\mathsf{r}})^{-1} (\hat{D}_{k}^{\mathcal{S},\mathsf{lr}})^{T} \Big),$$

$$M^{\mathsf{lr}} := \sum_{k=1}^{3} \Big( D_{k}^{\mathcal{S},\mathsf{ll}} (A^{\mathcal{K},\mathsf{l}})^{-1} (\hat{D}_{k}^{\mathcal{S},\mathsf{rl}})^{T} + D_{k}^{\mathcal{S},\mathsf{lr}} (A^{\mathcal{K},\mathsf{r}})^{-1} (\hat{D}_{k}^{\mathcal{S},\mathsf{rr}})^{T} \Big),$$

$$M^{\mathsf{rl}} := \sum_{k=1}^{3} \Big( D_{k}^{\mathcal{S},\mathsf{rl}} (A^{\mathcal{K},\mathsf{l}})^{-1} (\hat{D}_{k}^{\mathcal{S},\mathsf{ll}})^{T} + D_{k}^{\mathcal{S},\mathsf{rr}} (A^{\mathcal{K},\mathsf{r}})^{-1} (\hat{D}_{k}^{\mathcal{S},\mathsf{lr}})^{T} \Big),$$

$$M^{\mathsf{rr}} := \sum_{k=1}^{3} \Big( D_{k}^{\mathcal{S},\mathsf{rl}} (A^{\mathcal{K},\mathsf{l}})^{-1} (\hat{D}_{k}^{\mathcal{S},\mathsf{rl}})^{T} + D_{k}^{\mathcal{S},\mathsf{rr}} (A^{\mathcal{K},\mathsf{r}})^{-1} (\hat{D}_{k}^{\mathcal{S},\mathsf{rr}})^{T} \Big),$$

$$\bar{M}^{\mathsf{ll}} := \sum_{k=1}^{3} \Big( \bar{D}_{k}^{\mathcal{S},\mathsf{ll}} (A^{\mathcal{K},\mathsf{l}})^{-1} (\hat{D}_{k}^{\mathcal{S},\mathsf{ll}})^{T} + \bar{D}_{k}^{\mathcal{S},\mathsf{lr}} (A^{\mathcal{K},\mathsf{r}})^{-1} (\hat{D}_{k}^{\mathcal{S},\mathsf{lr}})^{T} \Big),$$

$$\bar{M}^{\mathsf{lr}} := \sum_{k=1}^{3} \left( \bar{D}_k^{\mathcal{S},\mathsf{ll}} (A^{\mathcal{K},\mathsf{l}})^{-1} (\hat{D}_k^{\mathcal{S},\mathsf{rl}})^T + \bar{D}_k^{\mathcal{S},\mathsf{lr}} (A^{\mathcal{K},\mathsf{r}})^{-1} (\hat{D}_k^{\mathcal{S},\mathsf{rr}})^T \right),$$

$$\bar{M}^{\mathsf{rl}} := \sum_{k=1}^{3} \left( \bar{D}_k^{\mathcal{S},\mathsf{rl}} (A^{\mathcal{K},\mathsf{l}})^{-1} (\hat{D}_k^{\mathcal{S},\mathsf{ll}})^T + \bar{D}_k^{\mathcal{S},\mathsf{rr}} (A^{\mathcal{K},\mathsf{r}})^{-1} (\hat{D}_k^{\mathcal{S},\mathsf{lr}})^T \right),$$

$$\bar{M}^{\mathsf{rr}} := \sum_{k=1}^{3} \left( \bar{D}_k^{\mathcal{S},\mathsf{rl}} (A^{\mathcal{K},\mathsf{l}})^{-1} (\hat{D}_k^{\mathcal{S},\mathsf{rl}})^T + \bar{D}_k^{\mathcal{S},\mathsf{rr}} (A^{\mathcal{K},\mathsf{r}})^{-1} (\hat{D}_k^{\mathcal{S},\mathsf{rr}})^T \right). \tag{106}$$

# References

[1] V.R. Ambati and O. Bokhove, Space-time discontinuous Galerkin discretization of rotating shallow water equations, *J. Comput. Phys.* **225**(2), 1233–1261, 2007.

[2] D.N. Arnold, F. Brezzi, B. Cockburn and L.D. Marini, Unified analysis of discontinuous Galerkin methods for elliptic problems, *SIAM J. Numer. Anal.* **39**(5), 1749–1779, 2002.

[3] K.J. Bai and J.W. Kim, A finite element method for free surface flow problems, *Theor. Appl. Mech.,* **1**(1), 1–27, 1995.

[4] J.T. Beale, A Convergent Boundary Integral Method for Three-Dimensional Water Waves, *Math. Comp.*, **70**, 977–1029, 2001.

[5] F. Brezzi, G. Manzini, D. Marini, P. Pietra and A. Russo, Discontinuous Galerkin approximations for elliptic problems, *Numer. Methods Partial Differential Eq.*, **16**(4), 365–378, 2000.

[6] J. Broeze, E.F.G. van Daalen and P. J. Zandbergen, A three-dimensional panel method for nonlinear free surface waves on vector computers, *Comput. Mech.*, **13**, 12–28, 1993.

[7] X. Cai, H.P. Langtangen, B.F. Nielsen and A. Tvieto, A finite element method for fully nonlinear water waves, *J. Comput. Phys.*, **143** 544–568, 1998.

[8] R.S. Johnson, A Modern Introduction to the Mathematical Theory of Water Waves, Cambridge University Press, Cambridge, 1997.

[9] J.W. Kim and K.J. Bai, A finite element method for two dimensional water wave problems, *Int. J. Numer. Methods Fluids,* **30**(1), 105–121, 1999.

[10] J.W. Kim, K.J. Bai, R.C. Ertekin, and W.C. Webster, A strongly-nonlinear model for water waves in water of variable depth – The irrotational Green-Naghdi model, *J. Offshore Mech. Arct. Eng.,* 125(1), 25–32.

[11] G. Klopman. M. Dingemans and E. van Groesen, A variational model for fully non-linear water waves of Boussinesq type, *Proceedings of 20th International Workshop on Water Waves and Floating Bodies*, Spitsbergen, Norway, 2005.

[12] M.S. Longuet-Higgins and E.D. Cokelet, The deformation of steep surface waves on water, I. A numerical method of computation, *Proc. Roy. Soc. London A*, **35**, 1–26, 1976.

[13] J.C. Luke, A variational principle for a fluid with a free surface. *J. Fluid Mech.*, **27**(2), 395–397, 1967.

[14] Q.W. Ma, G.X. Wu and R. Eatock Taylor, Finite element simulation of fully nonlinear interaction between vertical cylinders and steep waves. Part 2: Methodology and numerical procedure, *Int. J. Numer. Meth. Fluids*, **36**, 265–285.

[15] Q.W. Ma, G.X. Wu and R. Eatock Taylor, Finite element simulation of fully nonlinear interaction between vertical cylinders and steep waves. Part 1: Numerical results and validation, *Int. J. Numer. Meth. Fluids*, **36**, 287–308.

[16] Q.W. Ma and S. Yan, Quasi ALE finite element method for nonlinear water waves, *J. Comput. Phys.*, **212**, 52–72, 2006.

[17] S. McCormick, B. Briggs and V. Henson, *A multigrid tutorial*. SIAM, Philadelphia, 2000.

[18] J.W. Miles, On Hamilton's principle for surface waves, *J. Fluid Mech.,* **83**(1), 153–158, 1977.

[19] J.E. Romate and P.J. Zandbergen, Boundary integral equation formulations for free-surface flow problems in two and three dimensions, *Comput. Mech.,* 4(4), 1989.

[20] B. Satish, B. Kris, E. Victor, D.G. William, K. Dinesh, G.K. Matthew, McInnes C. Lois, B.F. Smith and Z. Hong, *PETSc users manual*, Argonne National Laboratory, NL-95/11 - Revision 2.1.5, 2004. `http://www-unix.mcs.anl.gov/petsc`

[21] B. Satish, B. Kris, D.G. William, K. Dinesh, G.K. Matthew, McInnes C. Lois, B.F. Smith and Z. Hong, *PETSc Web page*, 2001. `http://www.mcs.anl.gov/petsc`

[22] B. Satish, D.G. William, McInnes C. Lois and B.F. Smith, *Efficient Management of Parallelism in Object Oriented Numerical Software Libraries*, In Modern Software Tools in Scientific Computing by E. Arge, A.M. Bruaset and H.P. Langtangen, Birkhä user Press, 163–202. 1997.

[23] W. Tsai and D. Yue, Compuations of nonlinear free-surface flows, *Ann. Rev. Fluid Mech.,* **28**, 249–278, 1996.

[24] J.J.W. van der Vegt and S.K. Tomar, Discontinuous Galerkin Method for linear free surface gravity wave, *J. Sci. Comput.* **22**(1), 531–567, 2005.

[25] J.J.W. van der Vegt and H. van der Ven, Space-time discontinuous Galerkin finite element method with dynamic grid motion for inviscid compressible flows, *J. Comput. Phys.* **182**, 546–585, 2002.

[26] J.J.W. van der Vegt and Y. Xu, Space-time Discontinuous Galerkin Method for nonlinear water waves, *J. Comput. Phys.* **224**(1) 17–39, 2007.

[27] T. Vinje and P. Brevig, Numerical simulation of breaking waves, *Adv. Water Resources*, **4**, 77–82, 1981.

[28] J.H. Westhuis, The numerical simulation of nonlinear water waves in a hydrodynamic model test basin, Ph.D. thesis, University of Twente, Enschede, The Netherlands, 2001.

[29] G.B. Whitham, Linear and Nonlinear Waves, Wiley-Interscience, New York, 1974.

[30] G.X. Wu and R.E. Taylor, Finite element analysis fo two dimensional non-linear transient water waves, *Appl. Ocean Res.*, **16** 263–372, 1994.

[31] G.X. Wu and Z.Z. Hu, Simulation of nonlinear interactions between waves and floating bodies through a finite-element based numerical tnk, *Proc. R. Soc. Lond. Se. A* 460, 2797–2817, 2004.